Thin disks as sources of stationary axisymmetric electrovacuum spacetimes

Tomáš Ledvinka

Department of Theoretical Physics
Faculty of Mathematics and Physics
Charles University
V Holešovičkách 2, Praha 8, Czech Republic

A disertation submitted to the Faculty of Mathematics and Physics, Charles University, in accordance with the regulations for admission to the degree of Doctor of Physics.

Branch of the doctoral study: F-1 – Theoretical physics, astronomy and astrophysics

Praha, October 1998

Acknowledgements

I would like to thank professor Jiří Bičák for his help. He proposed an interesting problem, encouraged me in my work and he has always had the time to discuss my work with me, and has made valuable comments on the content of the thesis.

Contents

1 Introduction

Unlike in Newtonian gravity, there is a lack of complete exact solutions representing self-gravitating rotating compact objects in general relativity due to its essential non-linearity. On the other hand a great progress has been made within a class of the stationary axisymmetric vacuum or electro-vacuum asymptotically flat spacetimes where powerful methods were applied to obtain analytic solutions of Einstein's equations [1]. Among these solutions the most important role still plays the spacetime discovered by Kerr [2]. One of the reasons consists in the fact that compact astrophysical objects very often posses large specific angular momentum and a Kerr black hole is thus a natural candidate for the spinning remnant of gravitational collapse [3]. Indeed, assuming that the the cosmic censorship conjecture holds, the black–hole uniqueness theorems guarantee that the Kerr metric represents the unique solution describing all rotating vacuum black holes (cf. e.g. [4]). If one takes into account that the properties of the interior Schwarzschild solution describing a static spherically symmetric star surrounded by its gravitational field are even now, sixty years after its discovery, inspiring astrophysicists in a deeper understanding of the peculiarities of general relativity [5], there is no doubt that an exact interior Kerr solution would be even more exciting.

This, of course, has been realized by many workers. As the properties of *Kerr's spinning particle metric* were analyzed [6], [7], the search for such solution started (e.g. [8],[9]). Since that time several authors have been able to construct interior solutions that can be matched with the Kerr vacuum geometry as an external field, but the material of various balls or shells has very strange properties and allows no reasonable interpretation [10], [11], [12], [13]. For example, quite recent work, that appeared in 1991, gives "a toroidal source", consisting of "a toroidal shell ..., a disk ...and an annulus of matter interior to the torus" [14]. The masses of the disk and annulus are negative. The review on the "Sources for the Kerr Metric" [15], written in 1978, contains 71 references, and concludes with: "Destructive statements denying the existence of a material source for the Kerr metric should be rejected until (if ever) they are reasonably justified." To summarize in Hermann Bondi's way, the sources suggested so far for the Kerr metric are not the easiest materials to buy in the shops ...

In this situation less complicated sources should be studied – the most natural choice seems to be an axisymmetric thin disk. Even among such sources the most realistic one, the thin disk of a finite diameter without a radial pressure, was excluded from a list of possible sources of external parts of Kerr spacetime [16]. The situation is somewhat different in the special case of the *extreme* Kerr metric, where there is a definite relationship between mass and angular momentum. The numerical study [17] of uniformly rotating disks indicated how the extreme Kerr geometry forms around the disk in the "ultrarelativistic" limit. These numerical results were supported recently by the important analytical work [18]. If a re-

quirement of the finite diameter is relaxed, it can be shown that such disks can play a role of the interior Kerr solution with any angular momentum [19] (see also [20]).

In this thesis both our first results concerning Kerr disks and their generalization to stationary axisymmetric electro-vacuum spacetimes are presented. The section 2 is based on letter [19], published in 1993. The basic idea, which enables one to construct physically acceptable thin disks (as well as completely unreasonable shells) is then presented in section 3 in greater detail. Because we are interested in the interpretation of the stress-energy tensor of the disk using the 'usual' matter, we study only disks without radial pressure. Even though the radius of these disks is infinite, they have finite integral quantities such as mass or angular momentum, which means that their respective densities (as defined in section 4) have reasonable asymptotic behavior.

In the central region of the disk, the situation is quite complicated and the properties of the stress-energy tensor must be carefully studied using covariant characteristics – the energy conditions which are introduced in section 5. It is shown that for a general axisymmetric stationary electro-vacuum asymptotically flat spacetime which admits Weyl-Papapetrou coordinates the reasonable disk-like source may exist and that the surface stress-energy tensor of such a disk may consist of two counter-rotating streams of (charged electro-) geodesic particles at each radius, if certain conditions (studied in section 6) are met. Although in last years several galaxies were found to have the disks built from two nearly identical counter-rotationg stellar components (see e.g. [21]), the presence of counter-streaming component apparently makes such disks not so realictic astrophysically. Wee shall see, however, that the Kerr disks exist with the mass of the co-rotating component exceeding 90% of the total mass of the disk.

It is clear that physically realistic disks can be constructed only within certain limits of the values of total charge, angular momentum, effective radius of the disk, and other parameters which enter into the metric. The survey of the parameter space of the Kerr-Newman disks is presented in section 7. The analogous survey of Tomimatsu-Sato $\delta = 2$ disk sources is given in section 8. In these two sections the properties of disks generating considered spacetimes are studied with an emphasis on possible interpretations of the surface stress-energy tensor of the disk and on various relativistic phenomena, such as the existence of ergoregions or of closed timelike curves in the vicinity of the disks. In appendices A, B and C the plots of relevant disk quantities as functions of the circumferential radius are given.

2 Relativistic disks as sources of the Kerr metric

This section is based on letter [19], with several notes appended.

Bičák, Lynden–Bell and Katz [22] (BLK in the following) have shown that most vacuum *static* Weyl solutions can arise as the metrics of counter–rotating relativistic disks (see [22], also for other references on relativistic disks). The simple idea which inspired the work of BLK is commonly used in Newtonian galactic dynamics [23] (the idea first appeared in Kuzmin's work [24]): Imagine a point mass M placed at a distance b below the centre $\varrho = 0$ of a plane $z = 0$ (see Figure 1). This gives a solution of Laplace's equation above the plane. Then consider the potential obtained by reflecting this $z \geq 0$ potential in $z = 0$ so that a symmetrical solution both above and below the plane is obtained. It is continuous but has a discontinuous normal derivative on $z = 0$, the jump in which gives a positive surface density on the plane. In galactic dynamics one considers general line distributions of mass along the negative z–axis and, employing the method described above, one finds the potential–density pairs for general axially symmetric disks. In fact, Bičák, Lynden–Bell and Pichon [25] found an infinite number of new static solutions of Einstein's equations starting from realistic potentials used to describe flat galaxies, as given recently by Evans and de Zeeuw [26].

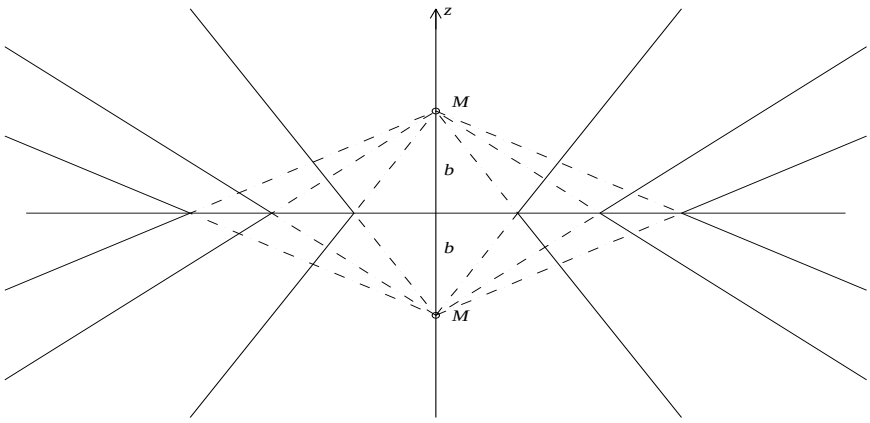

Figure 1: Gravitational field of a Kuzmin disk (illustrated using lines of force)

Here we wish to demonstrate that a similar method works also for axisymmetric, reflection symmetric, *stationary* spacetimes. It is important to realize that although now no metric function solves Laplace's equation as in the static case, we may view the procedure described above as the *identification* of the hypersurface $z = b$ with $z = -b$. The field then remains continuous but the jump of its normal derivative induces a matter distribution in the disk which arises due

to the identification. What remains to be seen, is whether the material can be "bought in the shops".

This idea can be employed for all known asymptotically flat stationary vacuum spacetimes, e.g. for the Tomimatsu–Sato solutions, for the "rotating" Curzon solution, or for other metrics (cf. [27] for references). Here we shall illustrate the procedure for the simplest, but most interesting case — the Kerr metric.

A stationary axisymmetric vacuum metric can be written in canonical coordinates (t, φ, ϱ, z) in the form [27]

$$ds^2 = f^{-1}\left[g\,(d\varrho^2 + dz^2) + \varrho^2 d\varphi^2\right] - f(dt + Ad\varphi)^2 \ , \tag{1}$$

where f, g, A are functions of ϱ, z (we put $c = G = 1$). Spheroidal coordinates (x, y) are commonly used, and we introduce both prolate ($\kappa = +1$) and oblate ($\kappa = -1$) ones since we wish to include all types of Kerr metrics:

$$z = \lambda xy \ , \ \varrho = \lambda\left[(x^2 - \kappa)(1 - y^2)\right]^{1/2} \ , \ \lambda = \text{const.} \ . \tag{2}$$

For the Kerr solution (mass M, specific angular momentum $a \geq 0$) the functions in (1) are ratios of polynomials [27]:

$$f \ = L/E \ , \qquad g \ = L/F \ , \quad A = B/L \ , \tag{3}$$

$$L = p^2x^2 + q^2y^2 - 1 \ , E = (px + 1)^2 + q^2y^2 \ , \tag{4}$$

$$F = p^2(x^2 - \kappa y^2) \ , \quad B = 2Mq(1 - y^2)(px + 1) \ , \tag{5}$$

$$\kappa p^2 + q^2 = 1 \ , \quad q = a/M \ , \quad \lambda = Mp \ . \tag{6}$$

Here $\kappa = 1$ for $a < M$, $\kappa = -1$ for $a > M$. If $a = M$, then $\kappa = 0$, $\lambda = M$, $p = q = 1$.

Now we identify the "planes" $z = b = \text{const.} > 0$ and $z = -b$ which will lead to disks with zero radial pressure. With the Kerr geometry the matching is more complicated than in the static cases and, therefore, we turn to Israel's covariant formalism (see [28] for its recent exposition). This enables us, using Einstein's field equations, to link the surface stress–energy tensor, $S_{(a)(b)}$, of the disk arising from this identification, to the jump $\left[K_{(a)(b)}\right] = K_{(a)(b)}|_{z=+b} - K_{(a)(b)}|_{z=-b}$ of normal extrinsic curvature across the timelike hypersurface Σ given by $z = b$ (or $z = -b$). The tetrad indices are denoted by (a), (b), ..., with the tetrad vectors being chosen so that three vectors tangent to Σ are just $e^{\mu}_{(a)} = \delta^{\mu}_{(a)}$ ($\mu = 0, 1, 2, 3$, $\{x^{\mu}\} = \{t, \varphi, \varrho, z\}$, $a = 0, 1, 2$), while $n^{\mu} = (0, 0, 0, 1/\sqrt{g_{zz}})$ is the unit normal.

As a consequence of Einstein's field equations we find the non–vanishing components of the surface stress–energy tensor to be

$$S_{(0)(0)} = \frac{ZLF}{E^2}\left(\frac{L'}{L} + \frac{F'}{F} - 2\,\frac{E'}{E}\right) \ ,$$

$$S_{(0)(1)} = \frac{ZBF}{E^2}\ \left(\frac{B'}{B} + \frac{F'}{F} - 2\,\frac{E'}{E}\right)\ , \tag{7}$$

$$S_{(1)(1)} = \frac{ZF}{L}\ \left[\varrho_1^2\left(\frac{L'}{L} - \frac{F'}{F}\right) + 2\,\frac{B^2}{E^2}\left(\frac{B'}{B} - \frac{E'}{E}\right)\right]\ ,$$

where L, E, F, B are given by (5), $\varrho_1^2 = \varrho^2 - B^2/E^2$,

$$Z = \frac{1}{16\pi}\ \left(\frac{E}{F}\right)^{1/2}\frac{2y_+}{\lambda(x^2-\kappa y^2)}\ , \quad y_+ = y|_{z=+b}\ , \tag{8}$$

and the operator "$'$" is defined by the relation $[f_{,z}]_{z=-b}^{z=b} = 2y_+ f'/\lambda(x^2-\kappa y^2)$ for any f. For the Kerr metric

$$\begin{aligned} L' &= 2x(p^2x^2 - q^2y^2 + 2q^2 - 1)\ , \\ E' &= 2p(x^2-\kappa)(px+1) + 2xq^2(1-y^2)\ , \\ F' &= 2x\left[p^2x^2 + (1-q^2)(y^2-2)\right]\ , \\ B' &= 2M(q/p)(1-y^2)\left[q^2 - (px+1)^2\right]\ . \end{aligned} \tag{9}$$

(In eqs. (8), (9), both x and y are evaluated at $z=b$; by inverting (2) one finds $x|_{z=+b} = x|_{z=-b}$, $y^2|_{z=+b} = y^2|_{z=-b}$.) Eqs. (7) – (9) give the stress–energy tensor of the disks.

Let us now show that the disks may be interpreted as being made of two streams of collisionless particles that circulate in opposite directions. In order to see this, we find, at each radius ϱ and for $z=b$, the preferred observer for whom the stress–energy tensor (7) acquires a diagonal form[1]. Let his 4–velocity (the timelike eigenvector of the tensor), read

$$V^\mu = N(1,\Omega,0,0)\ , \tag{10}$$

and his unit spatial base–vector in the φ–direction be

$$W^\mu = J(\beta,1,0,0)\ . \tag{11}$$

The conditions $V^\mu V_\mu = -1$, $W^\mu W_\mu = 1$, $V^\mu W_\mu = 0$ determine three of the parameters entering (10), (11) in terms of the fourth, of Ω say. Assume now a tensor $T^{\mu\nu}$ (which will be calculated from (7) – (9)) has non–vanishing components T^{00}, T^{01}, T^{11}. Then, by choosing

$$\Omega = \left\{(T_1^1 - T_0^0) - \left[(T_1^1 - T_0^0)^2 + 4\ T_1^0\ T_0^1\right]^{1/2}\right\}/2T_1^0\ , \tag{12}$$

[1]The question of existence of such observers was not addressed here. In section 5 we show, that it is related to the energy conditions and that, if $S_{(0)(0)}S_{(1)(1)} - S_{(0)(1)}^2 > 0$, V^μ is real vector.

$T^{\mu\nu}$ can be cast into the form

$$T^{\mu\nu} = \sigma V^\mu V^\nu + P W^\mu W^\nu \ , \tag{13}$$

where

$$\sigma = \frac{T^{00} - \beta^2 T^{11}}{N^2(1-\beta^2\Omega^2)} \ , \tag{14}$$

$$P = \frac{T^{11} - \Omega^2 T^{00}}{J^2(1-\beta^2\Omega^2)} \ . \tag{15}$$

Hence, the observers circulating with the 4–velocity (10) will see the diagonal form of $T^{\mu\nu}$ with

$$\begin{aligned} T^*_{(0)(0)} &= T^{\mu\nu}V_\mu V_\nu = \sigma \ , \\ T^*_{(0)(1)} &= T^{\mu\nu}V_\mu W_\nu = 0 \ , \\ T^*_{(1)(1)} &= T^{\mu\nu}W_\mu W_\nu = P \ . \end{aligned} \tag{16}$$

We call such observers "φ–isotropic" (ΦIOs) since the isotropy concerns the φ–direction only.

If $\sigma \geq P > 0$, ΦIOs can consider the stress–energy tensor (16) as representing two equal streams of collisionless particles that circulate in opposite directions with the *same* velocity

$$U^* = \left(\frac{P}{\sigma}\right)^{1/2} \ . \tag{17}$$

If σ_p is the surface proper rest mass density of one stream (measured in axes that move with it), then the surface density of its rest mass measured by an ΦIO is $\frac{1}{2}\sigma_0 = \sigma_p \left[1-(U^*)^2\right]^{-1/2}$. The surface energy density of the *pair* of streams is

$$T^*_{(0)(0)} = \sigma = \frac{\sigma_0}{\left[1-(U^*)^2\right]^{1/2}} = \frac{2\sigma_p}{1-(U^*)^2} \ . \tag{18}$$

The tangential pressure caused by the counter-rotation is $T^*_{(1)(1)} = \sigma (U^*)^2$. The sum of the proper rest mass surface densities of both streams is simply

$$2\sigma_p = \sigma - P \ . \tag{19}$$

The condition that the velocity of the streams U^* does not exceed the velocity of light is just the dominant energy condition (see e.g. [4]).

What is the relation of ΦIOs to the locally non–rotating frames (LNRFs)? ΦIOs *rotate* with respect to LNRFs with the velocity given by

$$V = \varrho^{-1}\, g_{\varphi\varphi}\, (\Omega - \omega) \ , \tag{20}$$

where $\omega = -g_{t\varphi}/g_{\varphi\varphi}$. Therefore, the streams circulate with *different* velocities in LNRFs and, of course, with respect to "distant stars". That is why the disks produce *stationary* rather than static fields.

The physical quantities introduced in (17) – (20) are given in terms of the metric (1) – (5), and the stress–energy tensor (7) – (9). Hence, *all the physical quantities describing the disks are given analytically.* The resulting expressions, however, are so complicated that it is only reasonable to exhibit them graphically. Yet, the *central* surface density has a simple form

$$\sigma_c = \frac{M}{2\pi} \frac{(b+M)^2 - a^2}{(b^2+a^2-M^2)^{1/2}\left[(b+M)^2+a^2\right]^{3/2}} \ . \tag{21}$$

In order for the central density to be positive, one must make the identification at $b^2 > M^2 - a^2$. (This is evident in the black–hole case since the hole's interior is mapped onto the rod $\varrho = 0$, $-(M^2-a^2)^{1/2} < z < (M^2-a^2)^{1/2}$.) If $a > M$, one has to choose $b > a - M$. The central density can become arbitrarily large for $b^2 \to (M^2-a^2)^{1/2}$ — a region "close" to the horizon (which itself was cut off) is then included. $\sigma_c > 0$ can be large also for $a \gtrsim M$. However, in the cases with $a > M$, it turns out that the physical condition $P \geq 0$ (cf. (17)) leads to the inequality

$$p^2(9x^4 - 6x^2 + 1) - p(4x^5 - 24x^3 + 4x) - (7x^4 - 10x^2 - 1) \leq 0 \ , \tag{22}$$

where $x = b/p$ and $p^2 = a^2/M^2 - 1$ (cf. (5)), which restricts b more strongly. For $a \gg M$ one finds $b_{min} \sim 9a^2/4M$. Then we can construct physical disks [2] only with $U^*_{max} \sim 0.3\ (M/a) \ll 1$.

In coordinates (ϱ, z) the ergoregion (cf. e.g. [4]) has a "toroidal" character, the center of the generating circle with $\varphi = \text{const.}$ is at $\varrho_0 = M(q - 1/2q)$, the radius being $\mathcal{R} = M/2q$. For $1 \geq a/M > 1/\sqrt{2} \doteq 0.707$, the disks given by $(M^2-a^2)^{1/2} < b < M^2/2a$ produce the ergoregion. Their central density is positive and the graphical results show (see below) that they are physical everywhere. It turns out that physical disks producing an ergoregion exist even for $a/M > 1$, provided that $a/M < 1.044$.

Here we shall confine ourselves to illustrate just one case — with $a/M = 0.8$. The disks corresponding to different choices of b are compared by exhibiting the circular velocities etc. as functions of the "circumferential" proper radius $R = \sqrt{g_{\varphi\varphi}}$, where $g_{\varphi\varphi}$ is given by (1) – (5). In Figure 2(a) we give the velocity curves of counter–rotating streams as measured by ΦIOs. These were calculated, starting from (17), for twelve disks; the disks become more relativistic with decreasing b.

[2] The "physical interpretation" means in this section counter-rotating streams of nongeodetic particles with equal opposite velocities with respect to ΦIO which satisfy energy conditions. It is the easiest generalization of the BLK disk model. If one would like to construct such disk model in a greater detail, the mechanism of exchange of radial momentum between the streams should be invented. In section 5 and 6 we distinguish between the energy conditions requirements (such as $P < \sigma$, which is equivalent to $V < 1$) and the existence of both (co- and counter-rotating) circular *geodesics.* This is given by radial behaviour of metric functions rather than altitudinal, which determines stress-energy tensor of the disk.

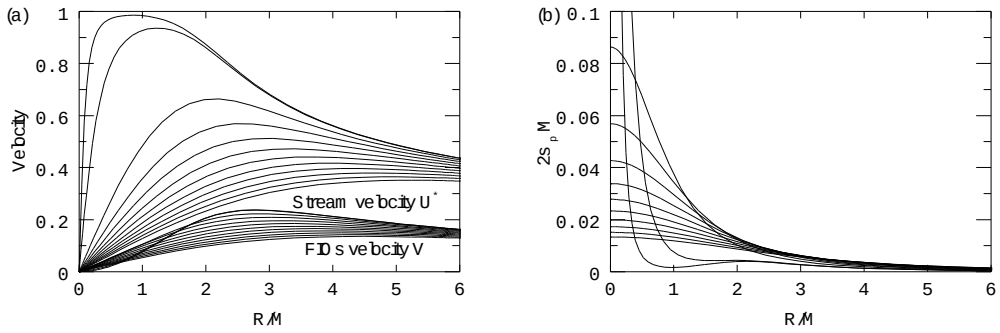

Figure 2: Velocity and density profiles of Kerr disks with $a/M = 0.8$

In the highly relativistic disks (upper two curves) U^* increases extremely rapidly as one moves away from the centre, approaching the velocity of light at $R \lesssim M$, and then start decreasing. Also in Figure 2(a) velocity curves of the ΦIOs with respect to the LNRFs are plotted by using (20). Although these velocities achieve also high values ($V \sim 0.25$), their maxima occur at larger $R \sim (2-3)M$. In particular, in the two most relativistic disks, the ΦIOs (the velocity curves of which cross the other curves from bottom to the top in Figure 2(b)) do not move so rapidly with respect to LNRFs *close* to the centre.(Here "close" refers to the proper circumferential radius R.) Just these two disks - from the twelve disks exhibited - produce an ergoregion.

Figure 2(b) gives the plots of the sum of the surface proper rest mass densities of both streams as calculated from (19). For highly relativistic disks, $2\sigma_p$ rises rapidly towards the centre; however, it decreases then very rapidly with R, and in the most relativistic case even reaches a local minimum at those R where $U^* \to 1$. The central gravitational redshift is $z_c \approx 10^3$ in this case.

We are not aware of any exact analytic solutions for the sources of the stationary gravitational fields with such physical properties as the disks constructed here. Although extending to infinity, they have finite mass and exhibit interesting relativistic properties like high velocities, large redshifts and dragging effects, including ergoregions. They may appear somewhat artificial astrophysically, but in the Newtonian limit - when no dragging arises - their features are the same [3] as for the rotating disks with only one stream of particles; in the relativistic regime, the central parts of a realistic, highly relativistic, rotating flattened object should have some properties in common with these disks.

[3] In fact even in the Newtonian gravity some counter-rotation is necessary if the disk should have prescribed values of mass and angular momentum, although the latter has no influence on the gravitational field. E.g. in zero angular momentum case corotating and counter-rotating component of the disk should have the same value of total angular momentum (with opposite sign).

3 Thin layers as sources of the stationary axisymmetric spacetimes

In this section we shall investigate the construction of the disk models in a greater detail and generality.

The easiest way to find a source producing a given stationary solution $\mathcal{M}_0$ of vacuum or electro-vacuum Einstein equations. It consists in glueing two exactly identical spacetimes ${}^{-}\mathcal{M} \equiv {}^{+}\mathcal{M} \subset \mathcal{M}_0$ together at their boundary hypersurface ${}^{\pm}S$. They are thus separated by a 3-dimensional layer of infinite δ-function type curvature which becomes the source of the spacetime (rather than various hidden or naked singularities). This method avoids the complicated problem of solving the interior field equations and matching the solution to the electro-vacuum solution outside.

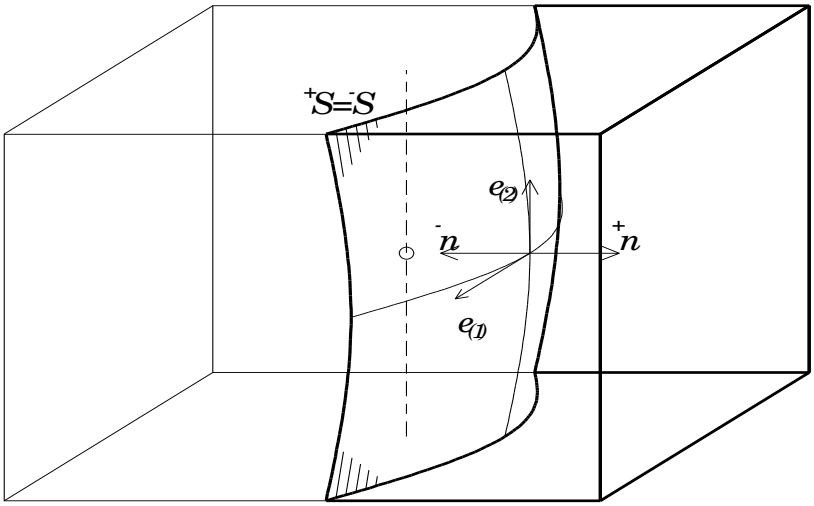

Figure 3: A part of a stationary spacetime $\mathcal{M}_0$ (depicted as a three-dimensional box with time coordinate omitted) and hypersurfaces ${}^{\pm}S$ delimiting the **emphasized** part which represents both ${}^{+}\mathcal{M}$ and ${}^{-}\mathcal{M}$

Three-dimensional hypersurfaces ${}^{\pm}S$ which will be identified (see Figure 3) may be characterized by two important quantities – the metric induced on them by external 4-metrics,

$$ {}^{\pm}g_{(a)(b)} = g_{\mu\nu}\, {}^{\pm}e^{\mu}_{(a)}\, {}^{\pm}e^{\nu}_{(b)} \tag{23} $$

($\mu, \nu = 0, 1, 2, 3$ and $a, b = 0, 1, 2$), and their extrinsic curvatures

$$ {}^{\pm}K_{(a)(b)} = {}^{\pm}e^{\mu}_{(a)}\, {}^{\pm}e^{\nu}_{(b)} \nabla_\mu\, {}^{\pm}n_\nu = -{}^{\pm}n_\nu\, {}^{\pm}e^{\mu}_{(a)} \nabla_\mu\, {}^{\pm}e^{\nu}_{(b)} \ . \tag{24} $$

Vectors ${}^{\pm}e^{\mu}_{(a)}, a = 0..2$ form the basis tangent to ${}^{\pm}S$ (in general not normalized) and unit vector ${}^{\pm}n^{\nu}$ is orthogonal to ${}^{\pm}S$ (i.e. ${}^{\pm}n^{\mu}\, {}^{\pm}n_\mu = 1$, ${}^{\pm}e^{\mu}_{(a)}\, {}^{\pm}n_\mu = 0$). Here ${}^{\pm}n^{\nu}$

are normals pointing from ${}^-\mathcal{M}$ to ${}^+\mathcal{M}$. The identification is admissible only if the induced metrics (23) are equivalent [29]. This is guaranteed by the fact that only the orientation of identified boundaries ${}^+S$ and ${}^-S$ is different, whereas basis vectors ${}^\pm e^\mu_{(a)}$ are identical. We will assume hypersurface ${}^+S$ to be prescribed by an equation $\Phi(x^\mu) = 0$ which yields the normal vector ${}^+n_\mu = \pm(\Phi_{,\alpha}\Phi^{,\alpha})^{-1/2}\ \Phi_{,\mu}$, where an appropriate sign must be chosen.

The jump in the extrinsic curvatures of ${}^+S$ and ${}^-S$ $\left[K_{(a)(b)}\right] = {}^+K_{(a)(b)} - {}^-K_{(a)(b)}$, determines the surface density of the stress-energy tensor by the relation [29]

$$S_{(a)(b)} = \frac{-1}{8\pi}\left([K_{(a)(b)}] - g_{(a)(b)}[K^{\ \ (c)}_{(c)}]\right). \tag{25}$$

Because whole spacetime is made of two identical copies, we have $[K_{(a)(b)}] = 2^+K_{(a)(b)}$.

Two commuting Killing vector fields of an stationary axisymmetric spacetime will be denoted ξ^μ and η^μ, η^μ having closed orbits. The coordinates associated with the Killing vectors will have their usual names, t and φ.

We exclude a case of the dynamic layer generating a stationary spacetime and assume that one of the basis vectors $e^\mu_{(0)}$ coincides with ξ^μ, and that the stationary basis $e^\nu_{(a)}$ is chosen, $\pounds_\xi e^\nu_{(a)} = 0$.

The resulting spacetime should have "reasonable" physical properties. One typical feature of an asymptotically flat spacetime is that at spatial infinity large 2-spheres surrounding the center have the ratio of the square of any circumference to the area of the sphere equal to π. To meet this requirement we will assume that the intersection of the boundary hypersurface S and hypersurface of constant time t is a smooth 2-surface ("the layer at given time"), which at infinity asymptotically approaches a plane we will denote $\mathcal{P}$, each part thus delimits the solid angle 2π.

The symmetries of the original spacetime $\mathcal{M}$ enable one to choose ${}^-\mathcal{M} = \mathcal{Q}\ {}^+\mathcal{M}$, where $\mathcal{Q}$ is some map preserving $g_{\mu\nu}$ and A_μ. For example let us assume that the original spacetime is stationary, axi- and reflection-symmetric Kerr solution with mass M and angular momentum $J = Ma$. If we introduce *some* (altitudinal) coordinate z related to the reflection symmetry and omit the time translation, the following symmetries can be used to obtain the ${}^-\mathcal{M}$ from ${}^+\mathcal{M}$.

$$z \ \rightarrow\ -z \tag{26}$$

$$\varphi \ \rightarrow\ \varphi + \delta \tag{27}$$

$$\varphi \ \rightarrow\ -\varphi \text{ and } a \ \rightarrow\ -a \tag{28}$$

Note that the z coordinate entering (26) may even be the latitudinal coordinate $\pi/2 - \vartheta$, where ϑ is one of Boyer-Lindquist's coordinates [7], as well as z coordinate of the original line element by Kerr [2], although we will prefer the

Weyl-Papapetrou z coordinate (29). The first symmetry (26), which enables one to identify ${}^{+}\mathcal{M}$ with its reflection symmetric copy, is illustrated in Figure 4a.

The other possible interpretation (Figure 4b) is based on composition of (27) and (28). If the boundary surface is reflection symmetric with respect to φ, it can be first rotated by angle π, which means that identification of points A and B' should be made. Then the symmetry (28) is plugged in and the natural identification of A and A' can be done, but one has to remember that both parts have opposite angular momentum parameter.

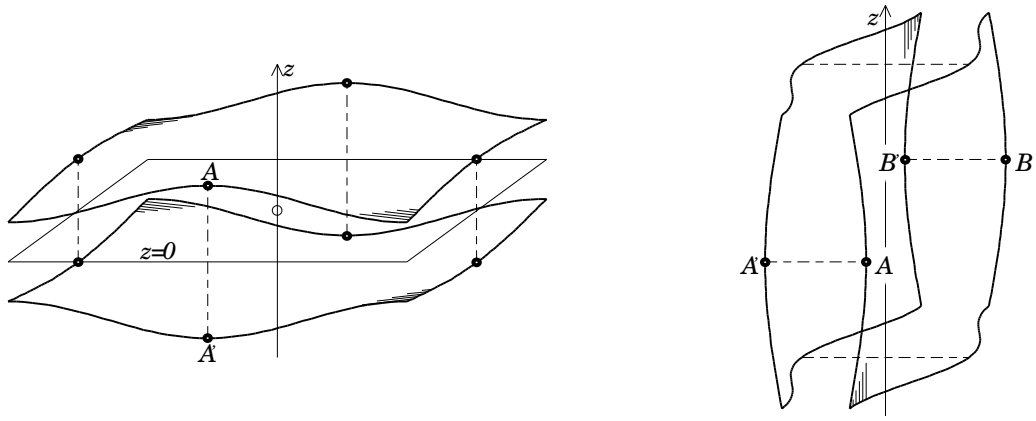

a) b)

Figure 4: Interpretations of the resulting spacetime based on – a) reflection b) axial – symmetry.

These two ways of identification are useful as an illustration of the method, but they do not alter the main idea that the resulting spacetime consists of two identical parts, and of a thin layer with the surface stress-energy tensor determined by the properties of the boundary hypersurface S. The new spacetime $\mathcal{M}$ need not necessarily be axially symmetric as a whole, if the asymptotical plane $\mathcal{P}$ is not parallel to the equatorial plane. This situation is illustrated in Figure 5, where the orientation of the angular momentum of both $\mathcal{M}_0$ and $\mathcal{M}$ is schematically presented before and after the identification. Complicated structure of the surface stress-energy tensor (no symmetry, too many nonvanishing components) yields no obvious interpretation. There may be another reason to prefer $\mathcal{P}$ to be parallel to the equatorial plane: If ${}^{+}S$ does not cross the equatorial plane, one can thing of $\mathcal{M}$ as an original spacetime $\mathcal{M}_0$ with removed equatorial region.

If stationary and axisymmetric electromagnetic potential of electro-vacuum spacetime is a linear combination of Killing vectors ξ^μ and η^μ, i.e. $A^{[\lambda}\xi^\mu\eta^{\nu]} = 0$, Maxwell tensor implies $R^t_t + R^\varphi_\varphi = 0$ and Weyl-Papapetrou (W-P) coordinates

$$ds^2 = e^{-2\nu}\left[e^{2\zeta}(d\varrho^2 + dz^2) + \varrho^2 d\varphi^2\right] - e^{2\nu}(dt + Ad\varphi)^2, \qquad (29)$$

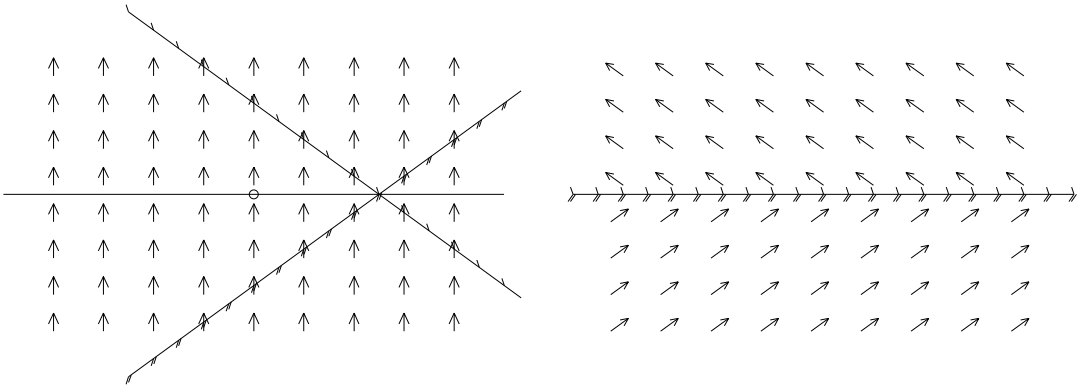

Figure 5: Orientation of the angular momentum before and after the identification, when $\mathcal{P}$ is tilted with respect to the equatorial plane.

may be introduced [4]. Even though the resulting spacetime is axially symmetric, its source – the surface stress-energy tensor $S_{(a)(b)}$ may not exhibit this symmetry. It depends on the shape of the hypersurface S. If S is tangential to the Killing vector field η^μ, i.e. if the orbits of η^μ are contained in this hypersurface, the basis vectors may be chosen such that $\pounds_\eta e^\nu_{(a)} = 0$, which ensures, that $S_{(a)(b)}$ is axially symmetric. Such sources will be called *disks*. This means that if $\xi^\mu n_\mu = \eta^\mu n_\mu = 0$, we can choose $e^\nu_{(0)} = \xi^\nu$ and $e^\nu_{(1)} = \eta^\nu$. Then if $e^\nu_{(2)}$ is chosen such that $g_{(0)(2)}$ and $g_{(1)(2)}$ vanish, the corresponding components $S_{(0)(2)}$ and $S_{(1)(2)}$ will cancel out and the only nonvanishing components of the surface stress-energy tensor of the disk are three diagonal components of $S_{(a)(b)}$ (energy density, and azimuthal and radial pressures) and one non-diagonal component $S_{(0)(1)}$ (angular momentum density).

A similar procedure is used to express electric charge and current density of the disk (for a general formalism for charged shells, see [30]). The projection of an electromagnetic vector potential into the boundary surfaces $A_{(a)} = e^\mu_{(a)} A_\mu$ has to be identical on both sides of the surface S; the electromagnetic field $F_{\alpha\beta}$ surrounding the disk is produced by the surface electric current density attached to the layer:

$$J_{(a)} = \frac{1}{4\pi} \left[F_{\mu\nu} e^\mu_{(a)} n^\nu \right] \tag{30}$$

If $e^\nu_{(0)} = \xi^\nu$, $e^\nu_{(1)} = \eta^\nu$ and $A^{[\lambda} \xi^\mu \eta^{\nu]} = 0$, this relation yields the stationary axisymmetric electric current with $J_{(2)} = 0$.

In our work we will use the hypersurface $\Phi(x^\mu) = z - b = 0$ which turns out to correspond to disks without radial pressure (for disks with radial pressure see [31]). Then

$$n^\mu = (g_{zz})^{-1/2} \delta^\mu_{(z)} \ , \tag{31}$$

and the simplest tangent basis is

$$e^\mu_{(a)} = \delta^\mu_{(a)} \ . \tag{32}$$

Since this choice makes $g_{(a)(b)} = g_{ab}$, we will not use brackets to distinguish projected and metric components but one has to remember that W-P coordinates must be applied to obtain correct results.

The fact that S is a surface of constant coordinate z implies simple formula for the extrinsic curvature, $K_{ab} = (g_{ab})_{,z} g_{\varrho\varrho}^{-1/2}/2$. The surface stress-energy tensor and electric current then turns out to be

$$S_{ab} = -\frac{\sqrt{g_{\varrho\varrho}}}{8\pi}\left(\frac{g_{ab}}{g_{\varrho\varrho}}\right)_{,z}, \tag{33}$$

$$J_a = -\frac{1}{2\pi}\frac{(A_a)_{,z}}{\sqrt{g_{\varrho\varrho}}}\ . \tag{34}$$

These formulae yield explicit expressions, after any stationary axisymmetric electro-vacuum exact solution $g_{\mu\nu}$, A_μ is plugged in. Unfortunately, they tend to be very long and so they will be explicitly given only in particular cases, e.g. $Q = M$, when some simplifications take place and resulting quantities have clear physical structure.

4 Total mass, angular momentum and charge

The considered method of construction of the disk sources guarantees that the values of integral parameters such as the total mass, angular momentum or charge are equal to those of the original spacetimes. The total quantities can also be obtained by integration of corresponding surface densities over the disk. If an electromagnetic field is present, the volume integral of electromagnetic energy density must also be considered.

In stationary asymptotically flat spacetime the mass M defined by asymptotic behavior of metric can be expressed as an integral of stress-energy tensor components over spacelike hypersurface Σ surrounding the regions of non-vanishing $T_{\mu\nu}$. The Komar mass integral (see e.g. [4]),

$$M = -\frac{1}{8\pi}\int\limits_{\partial\Sigma} \nabla^\mu \xi^\nu d\Sigma_{\mu\nu}\ . \tag{35}$$

over the 2-dimensional boundary of space-like hypersurface Σ, with ξ^ν being the timelike Killing vector, can be converted, using the Stokes' theorem, to the volume integral

$$M = \int_\Sigma (-2\ T_\mu{}^\nu + T^\sigma_{\ \sigma}\ \delta_\mu{}^\nu)\ \xi^\mu\ dS_\nu\ , \tag{36}$$

where $dS_\nu = \delta^t_\nu\ \sqrt{-g}\ d\varrho\ dz\ d\varphi$ is a volume element of hypersurface $t = const$. Since the surface stress-energy tensor S_{ab} is equivalent to surface distribution, the

total stress-energy tensor can be written as a sum of the regular (electromagnetic) part $\mathbf{T}_{\mu\nu}$ and the surface distribution proportional to $\delta(\bar{z})$

$$T_{\mu\nu} = \mathbf{T}_{\mu\nu} + e^a_\mu e^b_\nu S_{ab}\delta(\bar{z})/\sqrt{g_{zz}} \tag{37}$$

where $\bar{z} = z - b\,\mathrm{sgn}\,z$. Thus the Komar mass (36) consists of two components, the mass of electromagnetic field, M_E, and the mass of the fluid of the disk, M_D:

$$M_E = \int_\Sigma -2\mathbf{T}^t_t \sqrt{-g}\; d\varrho\; dz\; d\varphi\;, \tag{38}$$

$$M_D = \int_D (-2S^t_t + S^a_a)\sqrt{-g/g_{zz}}\; d\varrho\; d\varphi\;. \tag{39}$$

If disks without the radial pressure are considered ($S^\varrho_\varrho = 0$), and the line element (29), giving $g = -\varrho^2\; g_{\varrho\varrho}\; g_{zz}$, is used, the last integral reads

$$M_D = \int_D (S^\varphi_\varphi - S^t_t)\sqrt{g_{\varrho\varrho}}\; 2\pi\varrho\; d\varrho\;. \tag{40}$$

It is physically reasonable to use the proper circumferential radius $R = \sqrt{g_{\varphi\varphi}}$ for labeling the radial coordinate when depicting any radially dependent quantity in the disks. The surface density, μ_D, with respect to the circumferential radius may be defined by the relation

$$M_D = \int_D \mu_D\; 2\pi R\; dR \;=\; \int_D (S^\varphi_\varphi - S^t_t)\sqrt{g_{\varrho\varrho}}\,\frac{2\varrho}{g_{\varphi\varphi,\varrho}}\; 2\pi R\; dR\;. \tag{41}$$

This will enable us to compare mass density curves of various types of disks.

Using the surface stress-energy tensor (33), the mass of the disk can be determined by appropriate first derivatives of the metric:

$$M_D = \frac{1}{4\pi}\int g^{t\mu} g_{t\mu,z}\;\varrho\; d\varrho\; d\varphi\;. \tag{42}$$

This relation can be expressed in terms of the Weyl-Papapetrou metric potentials ν and A:

$$M_D = \frac{1}{2\pi}\int (\nu_{,z} + \frac{AA_{,z}}{2\varrho^2}e^{4\nu})\;\varrho\; d\varrho\; d\varphi\;. \tag{43}$$

Here the first term coincides with the Gauss law of Newtonian gravity $M_{Newt} = (4\pi)^{-1}\oint \nabla\nu.d\vec{S}$.

The integral expression for M_D (42) can be also derived directly from (35) if an appropriate limiting procedure is used because, after the identification is made, the antisymmetric tensor field $\nabla^\mu\xi^\nu$, which depends on first derivatives of the metric tensor, is no longer smooth. As the volume Σ containing the disk D is shrinking towards the disk, the integral (35) approaches M_D. The jump $[\nabla^\mu\xi^\nu]^{z=+b}_{z=-b}$, together with the surface element $d\Sigma_{\mu\nu}$, directly yields (42); so

the quantity M_D can be defined independently on the definition of S_{ab} and its interpretation as a distribution.

The total angular momentum in axisymmetric stationary spacetime can be defined by [4]

$$J = \frac{1}{16\pi} \int_{\partial\Sigma} \nabla^\mu \eta^\nu d\Sigma_{\mu\nu} \ , \tag{44}$$

where η^ν is the axial Killing vector field. The integral is equivalent with the volume integral over regions of non-vanishing $T_{\mu\nu}$:

$$J = \int_\Sigma T_\mu{}^\nu \eta^\mu dS_\nu \ . \tag{45}$$

Using the methods already mentioned, these integrals can be rewritten to the integral over the surface of the disk

$$J = \int_D S^t_\varphi \ \sqrt{g_{\varrho\varrho}} \ \varrho \ d\varrho \ d\varphi \ . \tag{46}$$

The last integral property of the disks to be considered here is the total charge

$$Q = \int J^t \ \sqrt{g_{\varrho\varrho}} \ 2\pi \varrho \ d\varrho \ . \tag{47}$$

All integral quantities can be used as independent checks of the code that evaluates S_{ab} and J_a.

5 Energy conditions and the interpretation of the surface stress-energy tensor of the disk

The energy conditions introduced in the studies of global properties of spacetimes (see e.g. [4]) are formulated in an invariant form and can be used when an invariant characterization of the surface stress-energy tensor $S_{\mu\nu}$ is needed. We will use the dominant and the weak energy conditions in order to find physically realistic sources. The weak energy condition requires, that any observer with her velocity W^μ must observe a nonnegative energy density $S_{\mu\nu}W^\mu W^\nu$. The dominant energy condition is based on the properties of the energy-momentum current $-S_{\mu\nu}W^\mu$ – this should be future directed timelike vector for classical matter. If this condition is satisfied, the weak energy condition holds.

The source which satisfies the energy conditions may still have an unclear physical interpretation. The next step consists in the diagonalization of $S_{\mu\nu}$. If the equation

$$(S_{\mu\nu} - \lambda g_{\mu\nu})X^\mu = 0 \tag{48}$$

has two real nonzero eigenvalues $-\mu$ and p and $-\mu \neq p$, the corresponding eigenvectors U^μ and V^μ can be rescaled into the form $U^\mu U_\mu = -1$, $V^\mu V_\mu = 1$,

because $U^\mu V_\mu = 0$. The equation (48) can be viewed as a diagonalization of the matrix defined by the mixed-indices tensor S^ν_μ which is no longer symmetric and has two different real eigenvalues corresponding to the energy density and azimuthal pressure, only if

$$(S^t_t - S^\varphi_\varphi)^2 + 4S^t_\varphi S^\varphi_t > 0 \ . \tag{49}$$

This inequality also implies that the disks which cannot be diagonalized must have $\det S_{AB} \leq 0$ $(A, B = t, \varphi)$.

The above procedure is equivalent to the transformation of $S_{\mu\nu}$ into the frame of an observer moving with the velocity U^μ so what

$$S_{\mu\nu} = \mu U_\mu U_\nu + p V_\mu V_\nu \ ; \tag{50}$$

here V^μ is the unit vector in azimuthal direction in observer's frame. We have called such an observer "the φ-isotropic observer" in section 2. If the decomposition (50) of $S_{\mu\nu}$ is possible, the weak energy condition is equivalent to

$$\mu \geq 0 \ \text{ and } \ p \geq -\mu \tag{51}$$

and the dominant energy condition reads

$$\mu \geq 0 \ \text{ and } \ |p| \leq \mu \ . \tag{52}$$

The eigenvectors U^μ and V^μ can also be used for the decomposition of the electric current inside the disk,

$$J^\mu = \sigma U^\mu + j V^\mu \ , \tag{53}$$

into the proper charge density σ and the current j, as measured by ΦIOs.

The diagonalization described above also yields a possible interpretation of the surface stress-energy tensor of the disks. Imagine that at each radius of the disk a massive circular ring is placed. Let it rotate with the velocity U^μ, its linear energy density is equal to the product of the proper surface density μ and its proper width. The ring is supported against the collapse or expansion by its internal azimuthal pressure p. Although usual materials do not provide $|p|/\mu \sim 1$, they are consistent with energy conditions and used not infrequently in general relativity. The material of such rings must be superconductive, if $j \neq 0$, and charged, when $\sigma \neq 0$ (this is consistent with the survey [32]). In the following section, however, we shall study more physical situations in which the stress tensor can be interpreted as counter-rotating streams of freely moving particles.

6 Disks formed of counter-rotating surface streams of charged particles

To interpret diagonal surface stress-energy tensor with two nonzero components S_{tt} and $S_{\varphi\varphi}$ placed in the equatorial plane of static axisymmetric spacetime Morgan and Morgan [33] introduced the disk created from counter-rotating surface circular streams of particles.

The most noticeable fact is that at a given radius the velocity of counter-rotating particles, which generate the azimuthal component of stress-energy tensor, and the velocity of a particle on circular geodesic on that radius are equal; this is so because the potentials satisfy the Einstein equations. To illustrate this coincidence we put $A = 0$ in (29). Then the angular velocities of the circular geodesic motion

$$\Omega_{1\pm} = \pm\sqrt{-\frac{g_{tt,\varrho}}{g_{\varphi\varphi,\varrho}}} = \pm\,\frac{e^{2\nu}}{\varrho}\sqrt{\frac{\varrho\nu_{,\varrho}}{1-\varrho\nu_{,\varrho}}} \tag{54}$$

and the angular velocities, which are needed to generate the S^{φ}_{φ} component of the surface stress-energy tensor

$$\Omega_{2\pm} = \pm\sqrt{\frac{S^{tt}}{S^{\varphi\varphi}}} = \pm\frac{e^{2\nu}}{\varrho}\sqrt{\frac{\zeta_{,z}}{2\nu_{,z}-\zeta_{,z}}}\ , \tag{55}$$

are equal because the vacuum Einstein equation

$$R_{\varrho z} = \frac{2\varrho\nu_{,\varrho}\nu_{,z}-\zeta_{,z}}{\varrho} = 0 \tag{56}$$

holds outside the disk.

The concept of counter-rotating streams can be extended to general stationary axisymmetric asymptotically flat electro-vacuum spacetimes with the reflection-symmetric metric and electromagnetic potentials entering (29). If the radial pressure component of the surface stress-energy tensor S_{ab} attached to the surface of identification vanishes (due to the choice $\Phi(x^{\mu}) = z - b = 0$), the possibility of construction of the disk from the surface streams of particles on circular orbits can be studied in the stationary case as well. The non-diagonal metric implies the non-diagonal surface stress-energy tensor and the counter-rotating streams can no longer have identical surface density and opposite velocities. If the electromagnetic field is present, it is generated by appropriate charges attached to the particles of both streams.

The two streams of charged dust moving in the plane of identification $z = \pm b$ are assumed to have the following energy-stress tensor and electric current:

$$S^{\alpha\beta} = \bar{\mu}_{+}U^{\alpha}_{+}U^{\beta}_{+} + \bar{\mu}_{-}U^{\alpha}_{-}U^{\beta}_{-}\ , \tag{57}$$

$$J^{\alpha} = \bar{\epsilon}_{+}U^{\alpha}_{+} + \bar{\epsilon}_{-}U^{\alpha}_{-}\ . \tag{58}$$

The circular orbits $U^\alpha_\pm = N_\pm[1,\Omega_\pm,0,0]^\alpha$ of both streams have to satisfy the radial force balance $\bar{\mu}U_{(\varrho);\alpha}U^\alpha = \bar{\epsilon}F_{(\varrho)\beta}U^\beta$. Due to the symmetries the covariant derivative simplifies and the equation of electro-geodesic motion for both streams reads

$$-\frac{1}{2}\bar{\mu}_\pm U^\alpha_\pm U^\beta_\pm g_{\alpha\beta,(\varrho)} = \bar{\epsilon}_\pm F_{(\varrho)\beta}U^\beta_\pm \ . \tag{59}$$

Since only the time and angular components of both the surface stress-energy tensor $S^{\alpha\beta}$ and the stream particle velocity $U^\mu_\pm$ are nonzero, only the following seven equations remain to be satisfied

$$\begin{bmatrix} S^{tt} \\ S^{\varphi t} \\ S^{\varphi\varphi} \end{bmatrix} = \mu_+ \begin{bmatrix} 1 \\ \Omega_+ \\ \Omega_+^2 \end{bmatrix} + \mu_- \begin{bmatrix} 1 \\ \Omega_- \\ \Omega_-^2 \end{bmatrix}, \tag{60}$$

$$\begin{bmatrix} J^t \\ J^\varphi \end{bmatrix} = \epsilon_+ \begin{bmatrix} 1 \\ \Omega_+ \end{bmatrix} + \epsilon_- \begin{bmatrix} 1 \\ \Omega_- \end{bmatrix}, \tag{61}$$

$$\frac{1}{2}\mu_\pm \left(g_{tt,\varrho} + 2g_{t\varphi,\varrho}\Omega_\pm + g_{\varphi\varphi,\varrho}\Omega_\pm^2\right) + \epsilon_\pm \left(F_{\varrho t} + F_{\varrho\varphi}\Omega_\pm\right) = 0 \ , \tag{62}$$

where $\epsilon_\pm = N_\pm\bar{\epsilon}_\pm$ and $\mu_\pm = N^2_\pm\bar{\mu}_\pm$.

Although for given energy-stress tensor and electric current, six quantities $\Omega_\pm$, $\epsilon_\pm$ and $\mu_\pm$ must be determined using these seven equations, the system is not over-determined because the following linear combination of (60)-(61)

$$\frac{1}{2}\left(g_{tt,\varrho}S^{tt} + 2g_{t\varphi,\varrho}S^{t\varphi} + g_{\varphi\varphi,\varrho}S^{\varphi\varphi}\right) + F_{\varrho t}J^t + F_{\varrho\varphi}J^\varphi \tag{63}$$

is equal to the sum of the left-hand sides of both equations (62).

So the disk can be described by the simple dust model (57) with electric current (58) only if the considered combination (63) is zero. This is true for any number of streams as long as each consists of electro-geodesic particles.

This is guaranteed by virtue of Einstein equations and the contracted Gauss-Codazzi equations, which result in the following relation (see e.g. [30])

$$-S^\beta_{\alpha;\beta} + F_{\alpha\beta}J^\beta = 0 \ , \tag{64}$$

where the left hand side of this equation is equal to (63). We can therefore discard one of the seven equations (60)-(62). If the third component of (60) is chosen the energy and charge densities can be expressed in a quite symmetric manner

$$\mu_\pm = \mp\frac{\Omega_\mp S^{tt} - S^{\varphi t}}{\Omega_+ - \Omega_-} \ , \tag{65}$$

$$\epsilon_\pm = \mp\frac{\Omega_\mp J^t - J^\varphi}{\Omega_+ - \Omega_-} \ . \tag{66}$$

This can be immediately substituted into (62) to obtain following system of two coupled equations for angular velocities of both streams:

$$\frac{1}{2}\left(\Omega_- S^{tt} - S^{\varphi t}\right)\left(g_{tt,\varrho} + 2g_{t\varphi,\varrho}\Omega_+ + g_{\varphi\varphi,\varrho}\Omega_+^2\right) + \left(\Omega_- J^t - J^\varphi\right)(F_{\varrho t} + F_{\varrho\varphi}\Omega_+) = 0$$
$$\frac{1}{2}\left(\Omega_+ S^{tt} - S^{\varphi t}\right)\left(g_{tt,\varrho} + 2g_{t\varphi,\varrho}\Omega_- + g_{\varphi\varphi,\varrho}\Omega_-^2\right) + \left(\Omega_+ J^t - J^\varphi\right)(F_{\varrho t} + F_{\varrho\varphi}\Omega_-) = 0 \quad (67)$$

This system of equations can be factorized to the product of cubic and quadratic equations. The roots of the cubic equation lead to unphysical, symmetric solutions with $\Omega_- = \Omega_+$. The quadratic equation

$$\begin{gathered}\Big(S^{tt\,2} g_{\varphi\varphi,\varrho} g_{tt,\varrho} + S^{tt} g_{\varphi\varphi,\varrho} J^t F_{\varrho t} - 2\, g_{t\varphi,\varrho} g_{\varphi\varphi,\varrho} S^{t\varphi} S^{tt} - J^t F_{\varrho\varphi} g_{\varphi\varphi,\varrho} S^{t\varphi} + S^{t\varphi\,2} g_{\varphi\varphi,\varrho}{}^2\Big)\Omega^2 + \\ \Big(2\, S^{tt} g_{t\varphi,\varrho} J^t F_{\varrho t} - 2\, J^\varphi F_{\varrho\varphi} S^{tt} g_{t\varphi,\varrho} + J^\varphi F_{\varrho\varphi} g_{\varphi\varphi,\varrho} S^{t\varphi} + 2\, S^{tt\,2} g_{t\varphi,\varrho} g_{tt,\varrho} - J^t F_{\varrho\varphi}{}^2 J^\varphi + \\ S^{tt} J^t F_{\varrho\varphi} g_{tt,\varrho} - S^{t\varphi} g_{\varphi\varphi,\varrho} J^t F_{\varrho t} + J^\varphi g_{\varphi\varphi,\varrho} S^{tt} F_{\varrho t} + 2\, S^{t\varphi\,2} g_{\varphi\varphi,\varrho} g_{t\varphi,\varrho} - \\ 2\, g_{t\varphi,\varrho} J^t F_{\varrho\varphi} S^{t\varphi} + J^{t\,2} F_{\varrho\varphi} F_{\varrho t} - 4\, S^{tt} g_{t\varphi,\varrho}{}^2 S^{t\varphi}\Big)\,\Omega + \\ J^{t\,2} F_{\varrho t}{}^2 + g_{\varphi\varphi,\varrho} S^{t\varphi} J^\varphi F_{\varrho t} - J^t F_{\varrho\varphi} J^\varphi F_{\varrho t} - 2\, g_{t\varphi,\varrho} J^t F_{\varrho t} S^{t\varphi} + S^{tt\,2} g_{tt,\varrho}{}^2 - \\ 2\, S^{tt} g_{t\varphi,\varrho} S^{t\varphi} g_{tt,\varrho} + g_{\varphi\varphi,\varrho} S^{t\varphi\,2} g_{tt,\varrho} + 2\, S^{tt} J^t F_{\varrho t} g_{tt,\varrho} - J^\varphi F_{\varrho\varphi} S^{tt} g_{tt,\varrho} = 0\end{gathered} \quad (68)$$

or its vacuum ($F^{\mu\nu} = 0$) limit,

$$g_{\varphi\varphi,\varrho}\Omega^2 + 2g_{t\varphi,\varrho}\Omega + g_{tt,\varrho} = 0\ , \quad (69)$$

which is the radial component of the usual equation of circular geodesic, determine the stream velocities. Both co-rotating and counter-rotating angular velocities $\Omega_\pm$ must be checked whether they represent time-like vectors. If two subluminal circular (electro-) geodesics exist, their orbital frequencies $\Omega_\pm$ can be substituted into (65-66). Physically acceptable are only positive stream densities $\bar{\mu}_\pm$, but we do not pose any restrictions on the sign of the charge density $\bar{\epsilon}_\pm$ or the value of the specific charge $\bar{\epsilon}_\pm/\bar{\mu}_\pm$.

The positivity of the stream densities $\mu_\pm$ (note that the *proper* densities are $\bar{\mu}_\pm$) is related to the sign of the determinant of the two by two matrix S^{AB} $(A, B = t, \varphi)$, because

$$\det S^{AB} = \varrho^{-4} \det S_{AB} = \mu_+\mu_-(\Omega_+ - \Omega_-)^2 = \mu p (U^t V^\varphi - U^\varphi V^t)^2\ . \quad (70)$$

If (57) is understood as the definition of a quadratic form on the two-dimensional vector space of covariant vectors, one finds the following statement trivial: Both stream densities $\bar{\mu}_\pm$ are positive, if $S^{AB}X_A X_B > 0$ for at least one two-component vector X_A, $\det S^{AB} > 0$ and two subluminal solutions $\Omega_\pm$ of (68) exist.

Each disk is characterized by the parameters of the original spacetime M,J,Q and the size b of the excluded region. The parameter b determines the "effective diameter" of the disk – this is the radius below which, e.g.,90% of the matter of the disk resides. It is clear that for large b, fields will be weak and the only

relativistic effects consist in the fact that the ratio of energy (as well as charge) densities (65-66) of both streams is governed by the metric potentials. This is not the case in Newtonian gravity where the angular momentum is not the source of dragging and only total angular momentum and charge of the disk are fixed. As b becomes smaller, the relativistic effects play more important role and the violation of energy conditions may occur. For set of spacetimes studied in the following, it was confirmed that unless the energy conditions are violated, *closed timelike curves do not exist in the spacetime surrounding the disk*. Disks compact enough, with parameters close to extreme black holes, exhibited the presence of the ergoregions in the vicinity of the disk but because at least one of $\Omega_{\pm}$ is tachyonic near the ergosphere, only disks made of rings are able to generate ergospheres outside.

The z-component of electro-geodesic equation

$$\frac{d^2z}{d\tau^2} = \frac{1}{2}g^{zz}g_{\mu\nu,z}U^{\mu}U^{\nu} + \frac{\bar{\epsilon}}{\bar{\mu}}F_{(z)\nu}U^{\nu} \tag{71}$$

determines the stability of an individual circular orbit. Particles slightly off the equatorial plane are returned back only if $\frac{d^2z}{d\tau^2}\Big|_{z=+b} < 0$. Because the issue of stability was not addressed in our work, this inequality was not studied within the parameter space of the disk sources of different (electro-)vacuum solutions discussed below.

7 Kerr-Newman disks

Although we already discused not only neutral dust disks but also the disks with electric currents we did not yet study explicitly their external fields. In this section we analyze disks producing Kerr-Newman metric.

To transform the Kerr-Newman metric from Boyer-Lindquist coordinates [7] t,r,ϑ,φ into Weyl-Papapetrou (W-P) coordinates (29) one can put

$$z = (r-M)\cos\vartheta \tag{72}$$

$$\varrho = \sqrt{(r-M)^2 + a^2 + Q^2 - M^2}\,\sin\vartheta \tag{73}$$

Resulting expressions are quite complicated unless the spheroidal coordinates

$$z = \sigma xy \tag{74}$$

$$\varrho = \sigma\sqrt{1-y^2}\sqrt{x^2-\kappa} \tag{75}$$

$$\sigma = \frac{Mp}{\delta}, \quad \delta = 1 \tag{76}$$

are used. The parameter $\kappa = 1, 0, -1$ discriminates dressed, extreme and naked solutions; and the parameter $p > 0$, the dimensionless charge $s = Q/M$, and

the dimensionless angular momentum $q = a/M$, are related by the equation $s^2 + q^2 + \kappa p^2 = 1$. The parameter $\delta = 1$ is included in the definition for further reference. In the extreme case ($s^2 + q^2 = 1$, $\kappa = 0$) this equations does not determine p and since in this case p appears in equations (83-86) only in the form of the product px the value of p can be chosen freely. The most natural choice is $p = 1$. The inverse transform

$$x = \frac{r_+ + r_-}{2\sigma} , \tag{77}$$

$$y = \frac{r_+ - r_-}{2\sigma\sqrt{\kappa}} , \tag{78}$$

where $r_\pm = \sqrt{\varrho^2 + (z \pm \sigma\sqrt{\kappa})^2}$ is not defined for $\kappa = 0$. For extreme black hole metrics transformation (78) has to be replaced by the usual polar coordinate formula $y = z/\sqrt{\varrho^2 + z^2}$ while (77) then simplifies to $x = \sqrt{\varrho^2 + z^2}/M$. Lines of constant x and y plotted in the plane $\varrho - z$ form ellipses and hyperbolas as showed in Figure 6.

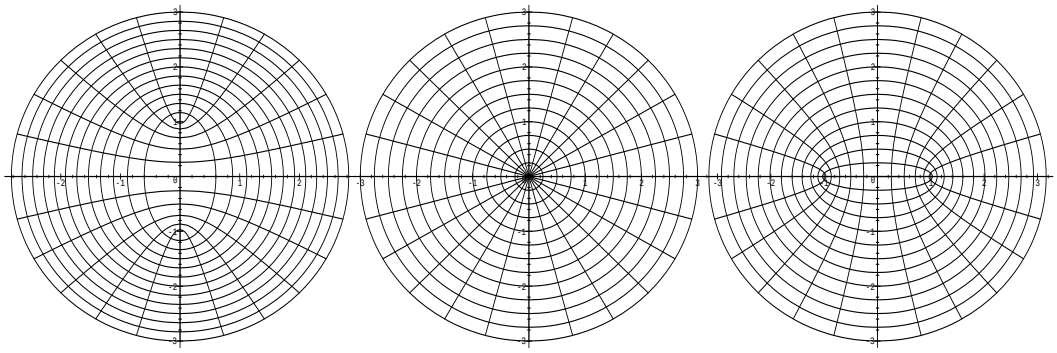

$\kappa = +1$ $\kappa = 0$ $\kappa = -1$

Figure 6: Prolate spheroidal, spherical and oblate spheroidal coordinate grid.

The spheroidal and Boyer-Lindquist coordinates have the following simple relation

$$r = \sigma x + M , \tag{79}$$

$$\cos\vartheta = y . \tag{80}$$

In Figure 7 the W-P coordinate grid $\varrho - z$ is plotted in Boyer-Lindquist coordinates. In this figure the region covered by W-P coordinates and the shape of surfaces $z = \pm b$ (and also the shape of region excluded by identification) are illustrated.

It is more convenient to express the operators $\frac{\partial}{\partial z}$ and $\frac{\partial}{\partial \varrho}$ using the inverse Jacobi matrix of (74-75), rather than differentiating the inverse map (77-78):

$$\frac{\partial}{\partial z} = \frac{1}{\sigma(x^2 - \kappa y^2)} \left[(x^2 - \kappa) y \frac{\partial}{\partial x} + x(1 - y^2) \frac{\partial}{\partial y} \right] , \tag{81}$$

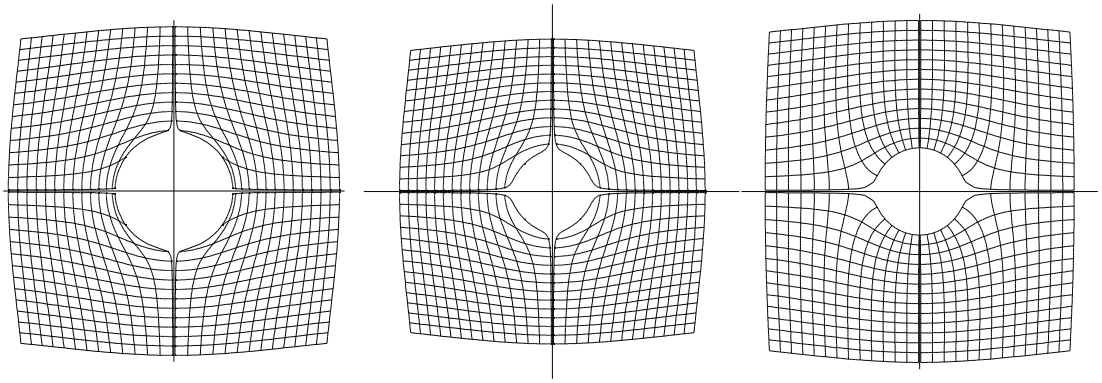

Figure 7: Planes $z = const.$ and cylinders $\varrho = const.$ in Boyer-Lindquist coordinates.

$$\frac{\partial}{\partial \varrho} = \frac{\varrho}{\sigma^2(x^2-\kappa y^2)}\left[x\frac{\partial}{\partial x} - y\frac{\partial}{\partial y}\right] . \tag{82}$$

The metric potentials of the Kerr-Newman spacetime expressed as functions of the radial and the latitudinal spheroidal coordinates x and y have the following form

$$e^{2\nu} = \frac{p^2x^2+q^2y^2+s^2-1}{(px+1)^2+q^2y^2} , \tag{83}$$

$$e^{2\zeta} = \frac{p^2x^2+q^2y^2+s^2-1}{p^2(x^2-\kappa y^2)} , \tag{84}$$

$$A = 2Mq(1-y^2)\frac{px-s^2/2+1}{p^2x^2+q^2y^2+s^2-1} . \tag{85}$$

The electromagnetic potential,

$$A_\mu dx^\mu = s(px+1)\frac{-dt+mq(1-y^2)d\varphi}{(px+1)^2+q^2y^2} , \tag{86}$$

yields the components of Maxwell tensor ($X = px+1$, $Y = qy$):

$$\begin{aligned}
F_{\varphi z} &= \tfrac{sqy}{Mp(X^2+Y^2)^2}\tfrac{1-y^2}{x^2-\kappa y^2}\left[2Xx(X^2+q^2)+p(x^2-\kappa)(X^2-Y^2)\right] ,\\
F_{\varphi\varrho} &= \tfrac{sq\varrho}{Mp^2(X^2+Y^2)^2}\tfrac{1}{x^2-\kappa y^2}\left[p(1-y^2)(X^2-Y^2)-2Xy^2(X^2+q^2)\right] ,\\
F_{zt} &= \tfrac{s}{Mp(X^2+Y^2)^2}\tfrac{y}{x^2-\kappa y^2}\left[p(X^2-Y^2)(x^2-\kappa)+2Xq^2x(1-y^2)\right] ,\\
F_{\varrho t} &= \tfrac{s\varrho}{M^2p^2(X^2+Y^2)^2}\tfrac{1}{x^2-\kappa y^2}\left[px(X^2-Y^2)-2XY^2\right] .
\end{aligned} \tag{87}$$

Using these formulae, the properties of stress-energy tensor distribution can be studied. Since the most general case includes a number of phenomena, to reveal their character, several special cases are discussed separately.

7.1 Schwarzschild disks

Metric coefficients of the Schwarzschild spacetime simplify to

$$g_{tt} = -\frac{x-1}{x+1} , \tag{88}$$

$$g_{\varphi\varphi} = \varrho^2 \frac{x+1}{x-1} , \tag{89}$$

$$g_{\varrho\varrho} = g_{zz} = \frac{(x+1)^2}{x^2-y^2} . \tag{90}$$

The resulting surface stress-energy tensor of the disk

$$S_a^b = -g^{bc}\frac{\sqrt{g_{\varrho\varrho}}}{8\pi}\left(\frac{g_{ac}}{g_{\varrho\varrho}}\right)_{,z} = \begin{pmatrix} S_t^t & 0 & 0 \\ 0 & S_\varphi^\varphi & 0 \\ 0 & 0 & 0 \end{pmatrix} = \frac{1}{1-V^2}\begin{pmatrix} -\mu & 0 & 0 \\ 0 & \mu V^2 & 0 \\ 0 & 0 & 0 \end{pmatrix} \tag{91}$$

$$\mu = \frac{Mb}{2\pi}\,\frac{R-M}{R+M}\,\frac{Mb^2+R^3}{(R^4-M^2b^2)^{3/2}} , \tag{92}$$

$$V^2 = \frac{MR(R^2-b^2)}{(R-M)(Mb^2+R^3)} , \tag{93}$$

$$2R = \sqrt{\varrho^2+(b+M)^2}+\sqrt{\varrho^2+(b-M)^2} \tag{94}$$

is studied in [22]. To interpret the stress-energy tensor authors consider a disk with two counter-rotating streams of particles with proper density $\mu/2$, which are counter-rotating with velocities $\pm V$. If the whole horizon of Schwarzschild black hole is contained in the removed region, i.e., if $b > M$, the velocities of particles creating the disk are subluminal, although for high central redshifts, particles on certain inner orbits are highly relativistic.

7.2 Extreme Reissner - Nordström disks

Metric coefficients of the extreme Reissner - Nordström spacetime read

$$g_{tt} = -\frac{x^2}{(x+1)^2} , \tag{95}$$

$$g_{\varphi\varphi} = \varrho^2\frac{(x+1)^2}{x^2} , \tag{96}$$

$$g_{\varrho\varrho} = g_{zz} = \frac{(x+1)^2}{x^2} , \tag{97}$$

and the fact that $g_{\varphi\varphi}/g_{\varrho\varrho} = \varrho^2$ implies that only one component of the surface stress-energy tensor is nonzero:

$$S_{tt} = \frac{x^2 y}{2\pi M(x+1)^4} . \tag{98}$$

Normal component of the electric field, $F_{zt} = M^{-1}\ y/(x+1)^2$, yields

$$J_t = -\frac{xy}{2\pi M(x+1)^3}\ . \tag{99}$$

This means that the proper mass density,

$$\mu = -S^t_t = \frac{M}{2\pi}\frac{b}{\sqrt{\varrho^2+b^2}(\sqrt{\varrho^2+b^2}+M)^2}\ , \tag{100}$$

and the proper charge density $\sqrt{-g^{tt}}J_t$ are identical and positive.

The disk consists of charged dust (non-)moving with four-velocity parallel to the Killing vector field ξ^μ. In these static disks electric repulsion is just counterbalanced with gravitational attraction – as in classical physics.

The contribution of the material of the disk to the total mass, i.e. the Komar integral (40),

$$M_D = b\ln\left(1+\frac{M}{b}\right)\ , \tag{101}$$

varies form 0 to M as b changes from 0 to ∞; the detailed dependence $M_D(b)$ is depicted in Figure 8. The fact that $M_D \to 0$ as $b \to 0$ means that the whole (Komar) mass of the extreme R-N black hole is equal to the energy stored in the electric field of the region covered by W-P coordinates (i.e. $r > M$, see (79) and Figure 7).

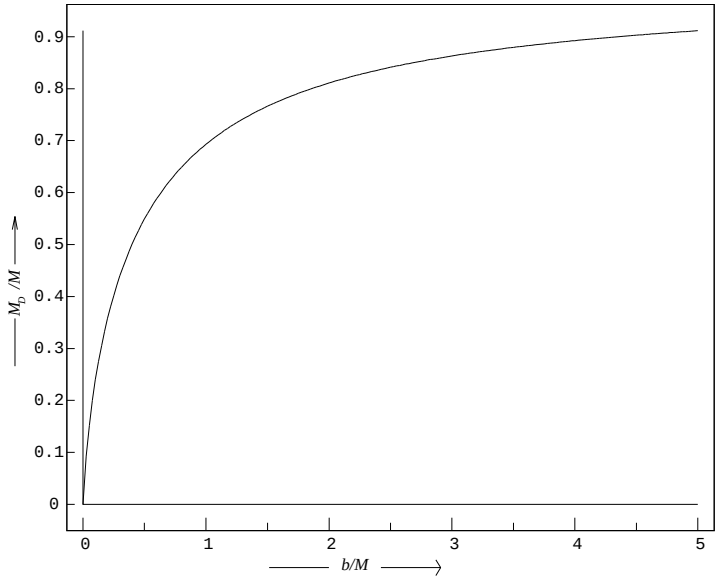

Figure 8: The dependence of of the mass of the disk M_D on the width of the excluded region b. The mass $M - M_D$ is of an electromagnetic origin.

7.3 Kerr disks

Because there are no restrictions on the sign or size of the specific charge attached to particles of both counter-rotating streams, all peculiarities of the interpretation of the disk concentrate on the properties of the the surface stress-energy tensor and the disks producing the Kerr spacetime exhibit the whole spectrum of behavior concerning the possibility to interpret a disk as physically realistic. The another reason to study the properties of the uncharged case is related to the astrophysical importance of the Kerr spacetime. The detailed description of the motivation to search for a realistic source of the Kerr spacetime was given in the first two sections.

Disks without the radial pressure generating Kerr spacetime are characterized by two dimensionless parameters, b/M and a/M, while the scale factor M can be omitted.

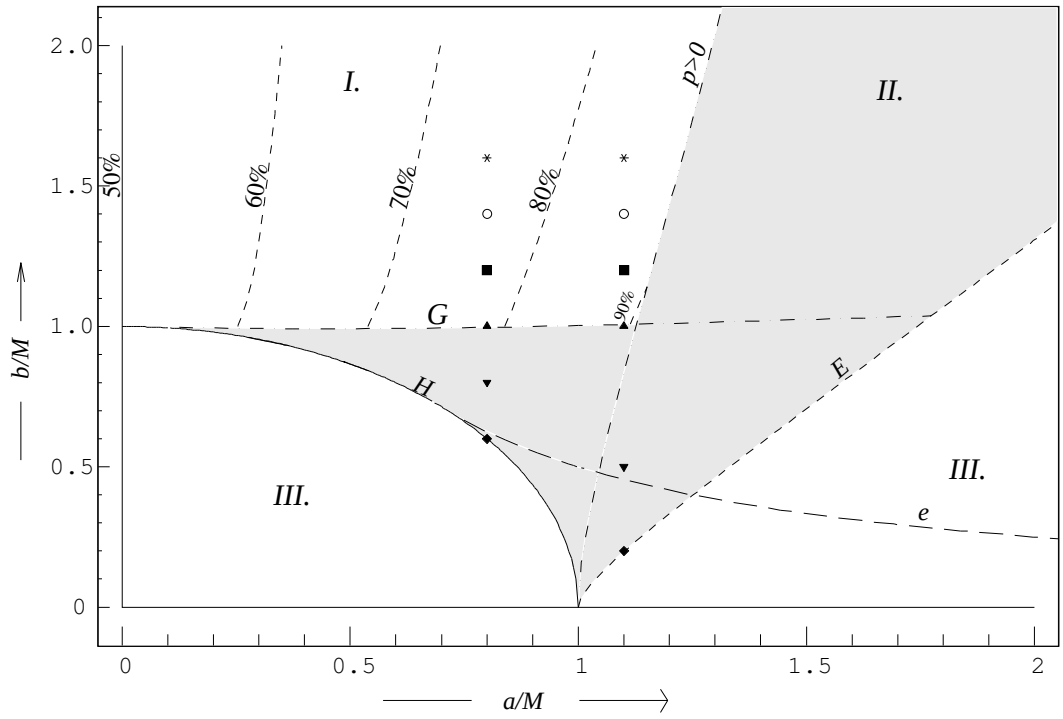

Figure 9: The parameter space of Kerr disks. I. Counter-rotating disks, II. Rings with azimuthal pressure, III. Energy conditions violated.

Only some regions in the parameter space of Kerr disks correspond to acceptable disks, which can be described as a counter-rotating material. In Figure 9 such regions are plotted. The horizontal dashed curve G which is almost identical with the line $b = M$ delimits the far region, where both solutions $\Omega_{\pm}$ correspond to subluminal velocities, from the near one, where the counter-rotating streams decomposition is not possible. Below this line the stress-energy tensor can be

diagonalized, but the role of the source play massive rings rotating with the velocity of ΦIOs. They must sustain positive or negative pressure. Because both densities of counter-rotating streams must be positive, the geodesic particle interpretation is possible only in the region left to the line labeled $p > 0$ (see (70)). Below the line E both energy conditions are violated at some radius of the disk as well as below the line H where the disk hits the horizon of the black hole. Using small circles, squares, etc., several disks with $a/M = 0.8$ and $a/M = 1.1$ are labeled. Radial properties of their relevant physical quantities are summarized in Appendix A. Finally below the dashed line e toroidal ergoregion is present near the center of the disk. The relation of the ergosphere of the Kerr black hole to the toroidal ergoregion of the disk spacetime is schematically depicted in Figure 10.

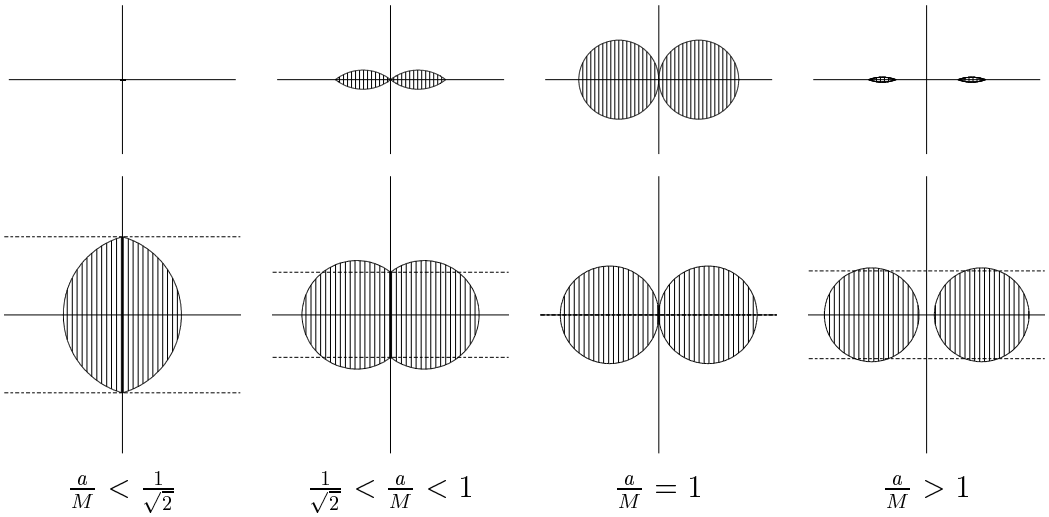

Figure 10: The relation of the ergosphere of the black hole (or the ergo-torus in the naked case) to the toroidal ergoregion of the spacetime of the disk before and after the identification. The planes of identification (i.e. the excluded region) are represented by the horizontal lines, their position represents a typical case when energy conditions considered are fulfilled. If $a = M$ there is no minimal "size" of the excluded region needed to guarantee the energy conditions.

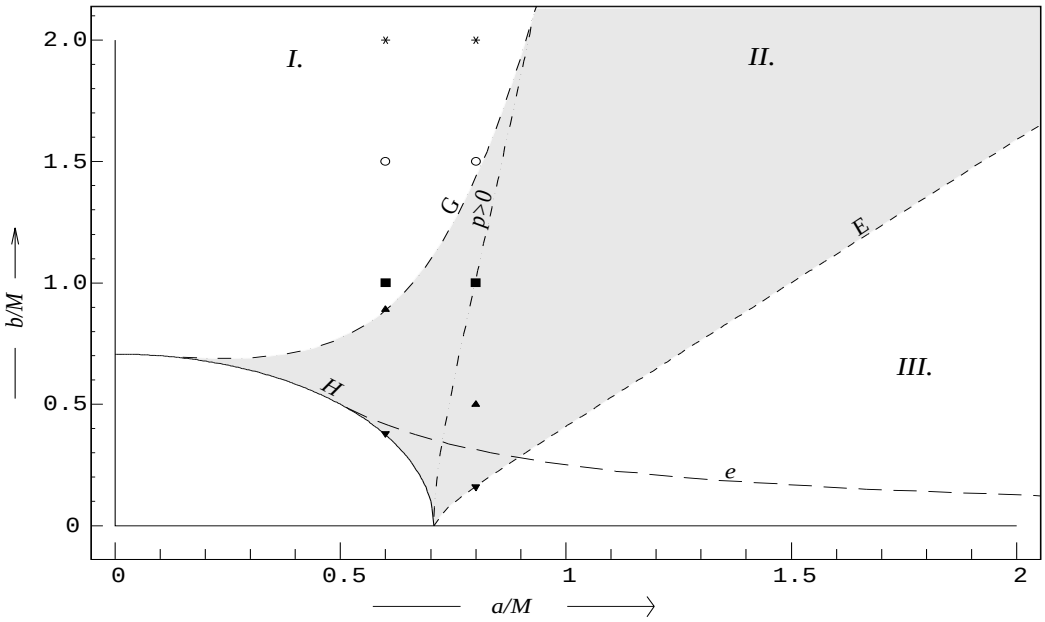

Figure 11: The parameter space of Kerr-Newman disks with $Q = M/\sqrt{2}$. I. Counter-rotating disks, II. Rings with azimuthal pressure, III. Energy conditions violated.

7.4 Charged (Kerr-Newman) disks

In the general case, all expressions become quite long and the only formulae worth displaying are the central energy and charge density of the disk

$$\mu_c = \frac{M}{2\pi}\frac{(b+M)^2 - a^2 - Q^2(1+b/M)}{[(b+M)^2+a^2]^2}\sqrt{\frac{(b+M)^2+a^2}{b^2+a^2+Q^2-M^2}}\ , \tag{102}$$

$$\epsilon_c = \frac{Q}{2\pi}\frac{(b+M)^2 - a^2}{[(b+M)^2+a^2]^2}\sqrt{\frac{(b+M)^2+a^2}{b^2+a^2+Q^2-M^2}}\ . \tag{103}$$

Because both the electrostatic and centrifugal forces are acting against the gravity, and the extreme Reissner - Nordström disks exhibit equilibrium of gravitational and electrostatic forces, one can conclude, that the region in the $a/M - b$ plane within the parameter space (see Figure 11), where disks can be made from counter-rotating electrogeodesic particles, is shrinking towards the line $a = 0$ as $Q \to M$. There are no such disks for $Q > M$, although the energy conditions may be fulfilled if b is large enough. Then the disk may be constructed from charged superconductive rings rotating with the velocity of Φ-isotropic observers.

8 Tomimatsu-Sato spacetimes

To illustrate the possibility of generating disk-like sources for arbitrary stationary axisymmetric vacuum spacetime, the properties of the disk sources of Tomimatsu-Sato $\delta = 2$ (TS2) spacetimes will be discussed in this section. This is a natural choice because the Kerr geometry is a member of TS family with the parameter $\delta = 1$.

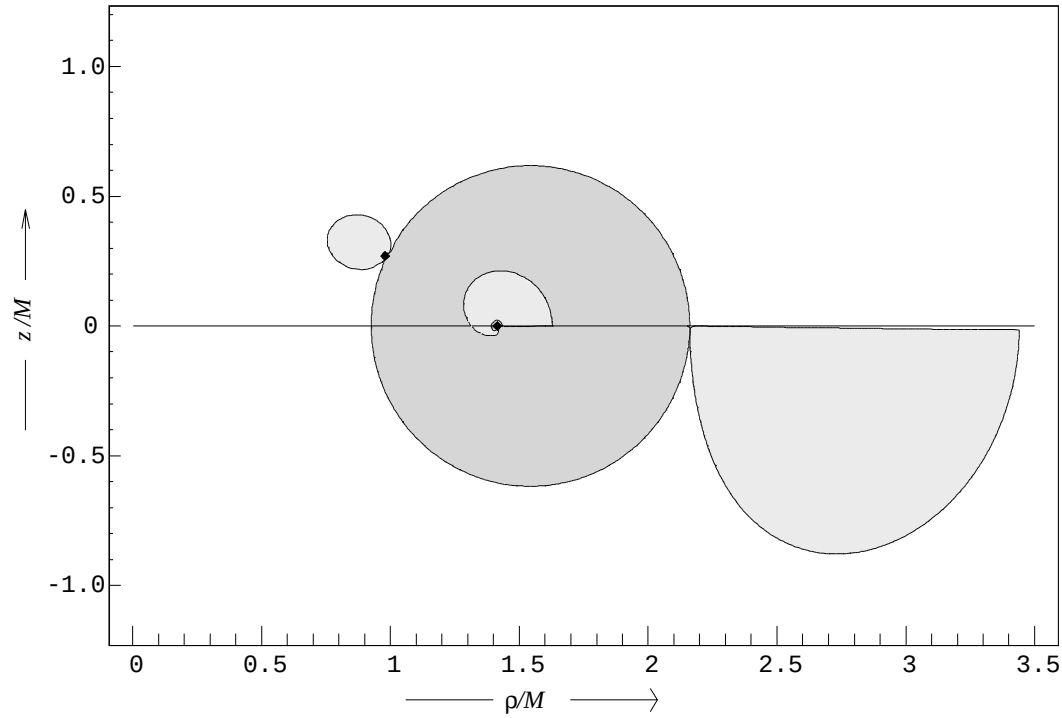

Figure 12: Ergoregion (dark grey) and regions of closed timelike curves (light grey) for $q = 3$. In this figure points below the plane $z = 0$ correspond to points with $x < 0$ and $y > 0$ and they represent TS2 solution in the region $r < M$.

TS2 spacetime is determined by the mass M and angular momentum M^2q [34]. The parameter p again satisfies the relation $\kappa p^2 + q^2 = 1$ and $\kappa = \pm 1$. Introducing the abbreviations $a = x^2 - \kappa$ and $b = 1 - y^2$, the line element is given by (29) where

$$
\begin{aligned}
e^{2\nu} &= \frac{p^4a^4 + q^4b^4 - 2p^2q^2ab(2a^2 + 2b^2 + 3\kappa ab)}{(\kappa p^2(x^4-1) - q^2(1-y^4) + 2px\kappa a)^2 + 4q^2y^2(px\kappa a + (px+1)b)^2}\ , \\
e^{2\zeta} &= \frac{p^4a^4 + q^4b^4 - 2p^2q^2ab(2a^2 + 2b^2 + 3\kappa ab)}{p^4(x^2 - \kappa y^2)^4}\ , \qquad (104) \\
A &= 2Mqb\frac{p^3xa(2(x^4-1)+(\kappa x^2+3)b)+(4ax^2+(3\kappa x^2+1)b)ap^2-(px+1)q^2b^3}{p^4a^4 + q^4b^4 - 2p^2q^2ab(2a^2 + 2b^2 + 3\kappa ab)}\ .
\end{aligned}
$$

These metric potentials are written down in the short form which does not include the extreme ($q = 1$) case; this is identical with the extreme Kerr metric. On the other hand the static limit of TS2 spacetime is the Darmois solution (Weyl metric with the metric potential ν proportional, with factor 2, to the metric potential of the Schwarzschild solution with the mass $M/2$), and the corresponding disk source are thus studied as a special case of Zipoy-Vorhees metrics in [22].

One of the most important differences between Kerr and TS2 family is that there remain both singular rings and toroidal regions of closed timelike curves in the region covered by W-P coordinates. Their shape is illustrated in Figure 12 for TS2 spacetime with $a/M = 3$.

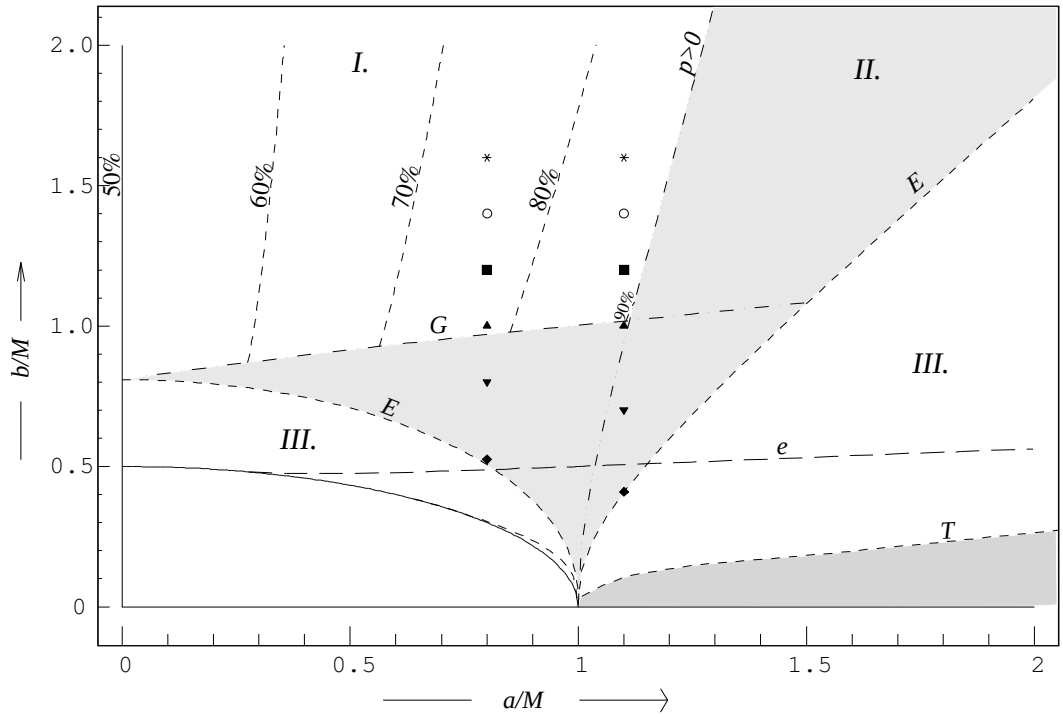

Figure 13: The parameter space of TS2 disks. I. Counter-rotating disks, II. Rings with azimuthal pressure, III. Energy conditions violated.

In Figure 13 the parameter space of TS2 disks is presented. Its structure is more complicated than in the Kerr case, because of previously mentioned phenomena. Disks with $a > M$ and sufficiently small b (those lying bellow the curve T) are surrounded by a toroidal region of closed timelike curves and the ring singularity may appear for even smaller b. As shown in Figure 13, such disks violate energy conditions. When $a < M$ the dominant energy condition is violated for disks with final central redshifts, which is not the case for the Kerr disks.

9 Concluding remarks

For a wide class of stationary axisymmetric electro-vacuum spacetimes we have shown a possibility to construct disk-like "interior solutions". These sources provide nice illustration of the well known fact that the Einstein equations govern not only the behavior of the gravitational field but also yield equations of motion for the matter. Thus, if a stress-energy tensor with a non-negative azimuthal and vanishing radial pressure is obtained by a removal of the equatorial region of spacetime considered, and two counter-rotating circular geodesics exist in the plane of the disk, the disk may be formed by assigning appropriate energy and charge densities to both counter-rotating streams. It is generally observed that such interpretation is allowed as long as the width of the excluded region is large enough and the gravitational attraction is stronger than electric repulsion. If the effective radius of the disk is small, it is not possible to construct disks with large a/M. In the astrophysically most plausible models, around 90% of the total mass of the disk of dust is rotating in one direction along geodesics and only 10% of the mass moves along counter-rotating geodesics.

Appendix A Radial properties of Kerr disks

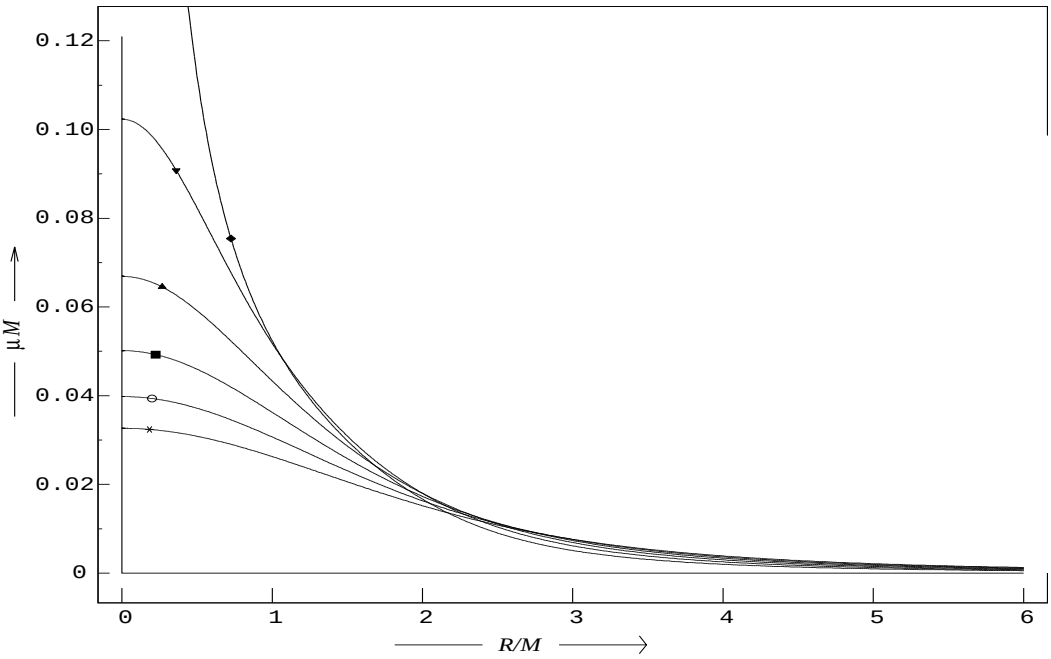

Figure 14: Energy density as seen by ΦIOs ($a/M = 0.8$)

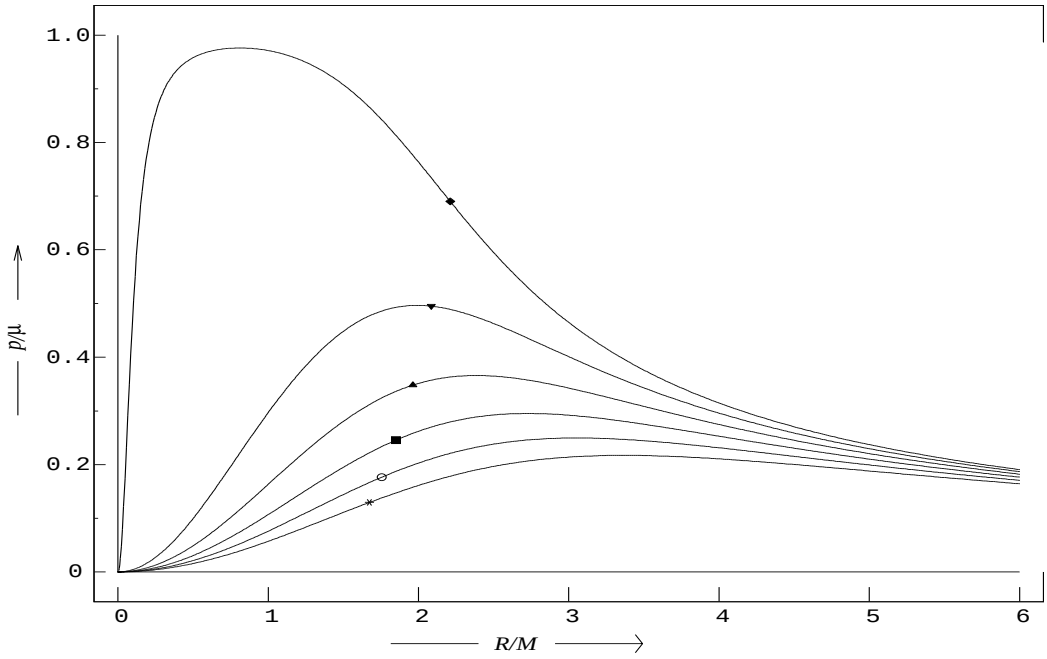

Figure 15: The ratio of the stress to the energy density as seen by ΦIOs ($a/M = 0.8$)

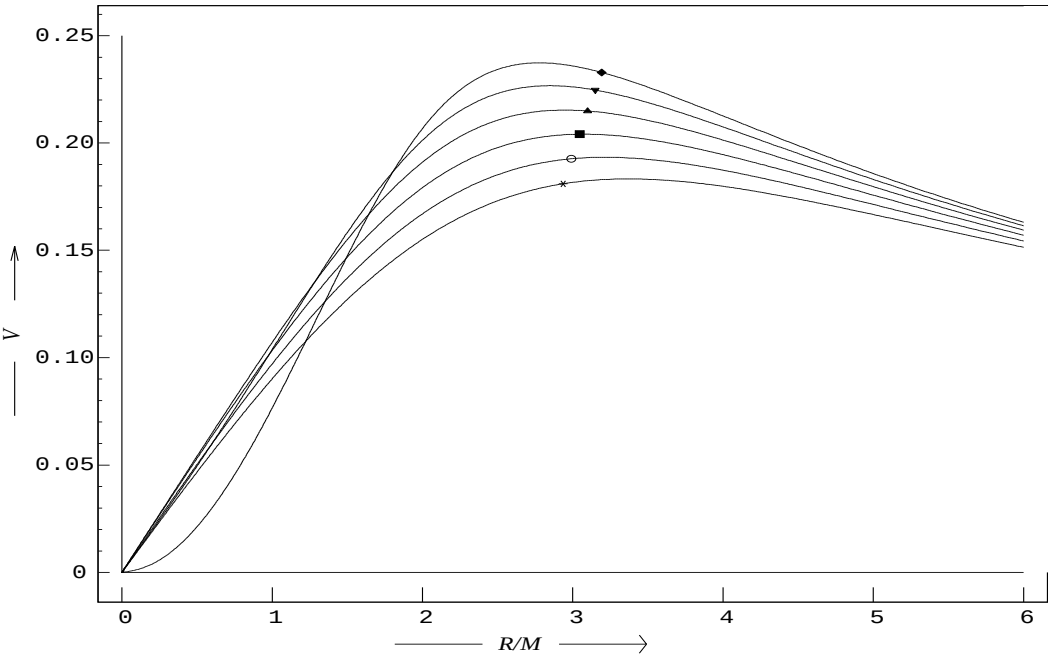

Figure 16: Velocity of ΦIOs with respect to LNRFs ($a/M = 0.8$)

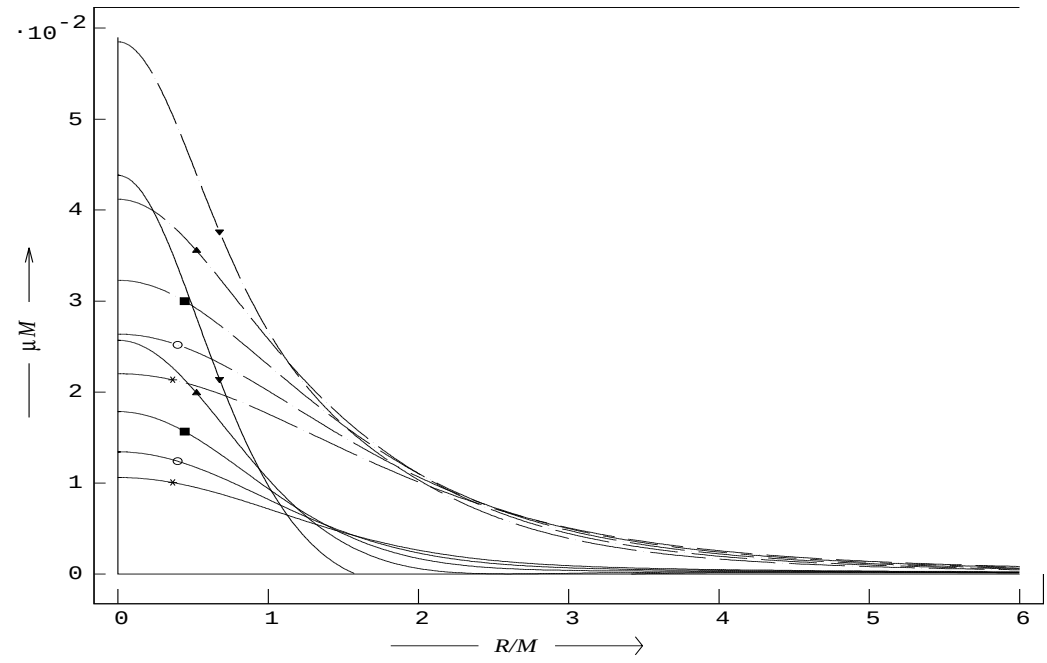

Figure 17: Energy density of both counter-rotating streams ($a/M = 0.8$)

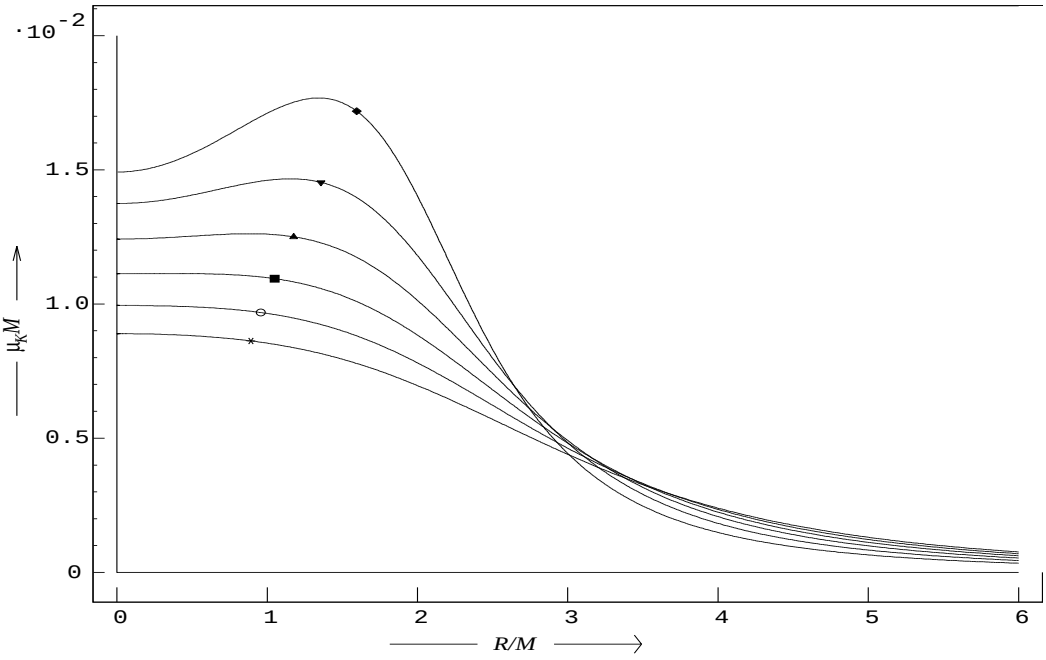

Figure 18: Komar mass density ($a/M = 0.8$)

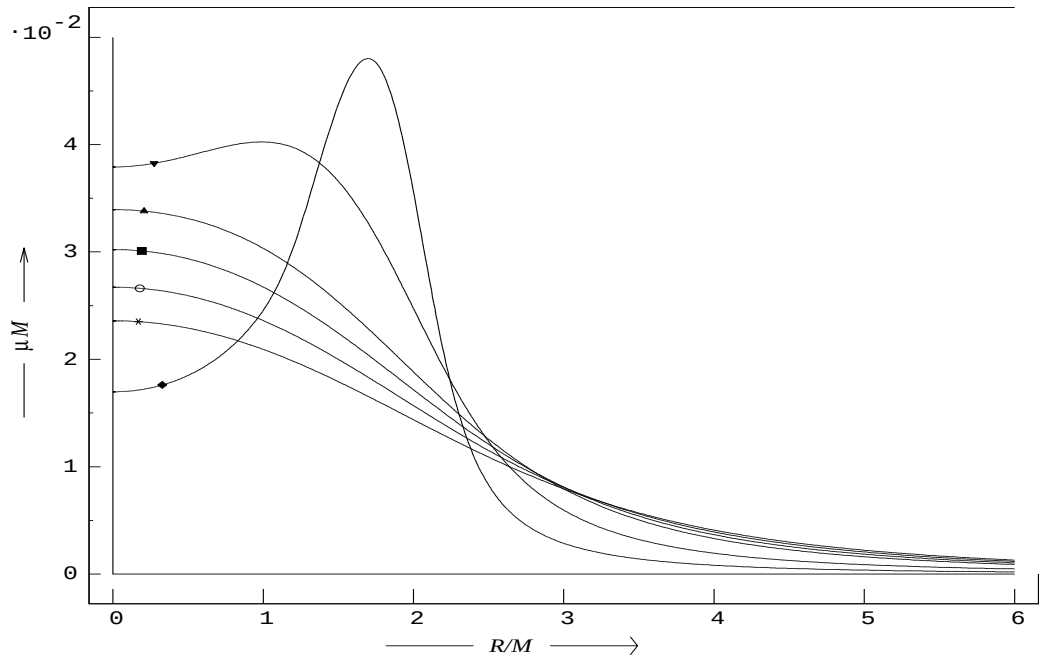

Figure 19: Energy density as seen by ΦIOs ($a/M = 1.1$)

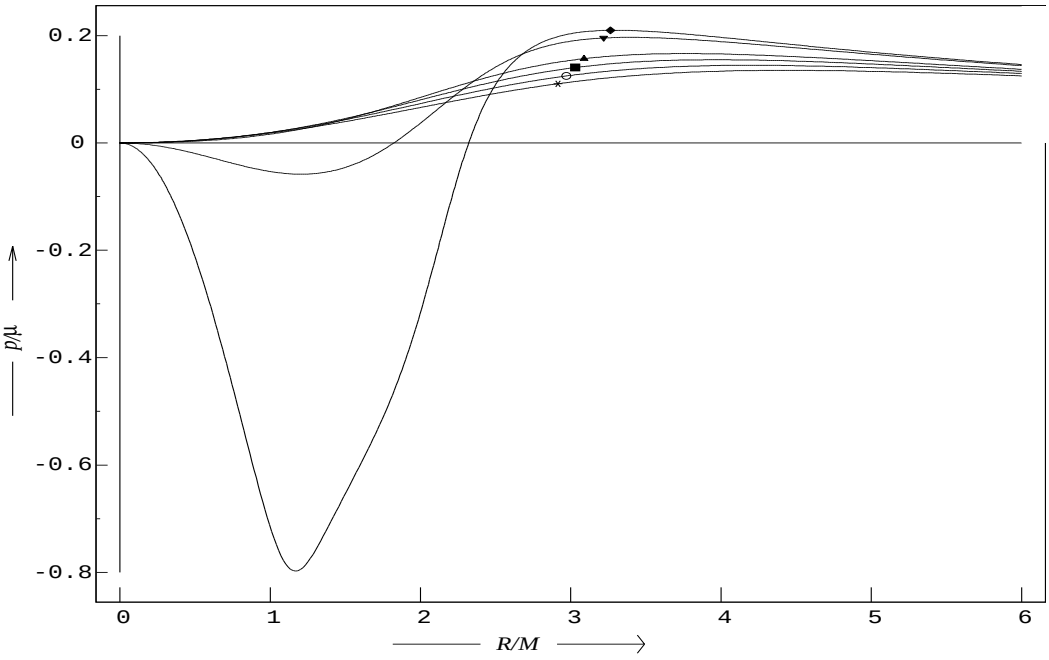

Figure 20: The ratio of the stress to the energy density as seen by ΦIOs ($a/M = 1.1$)

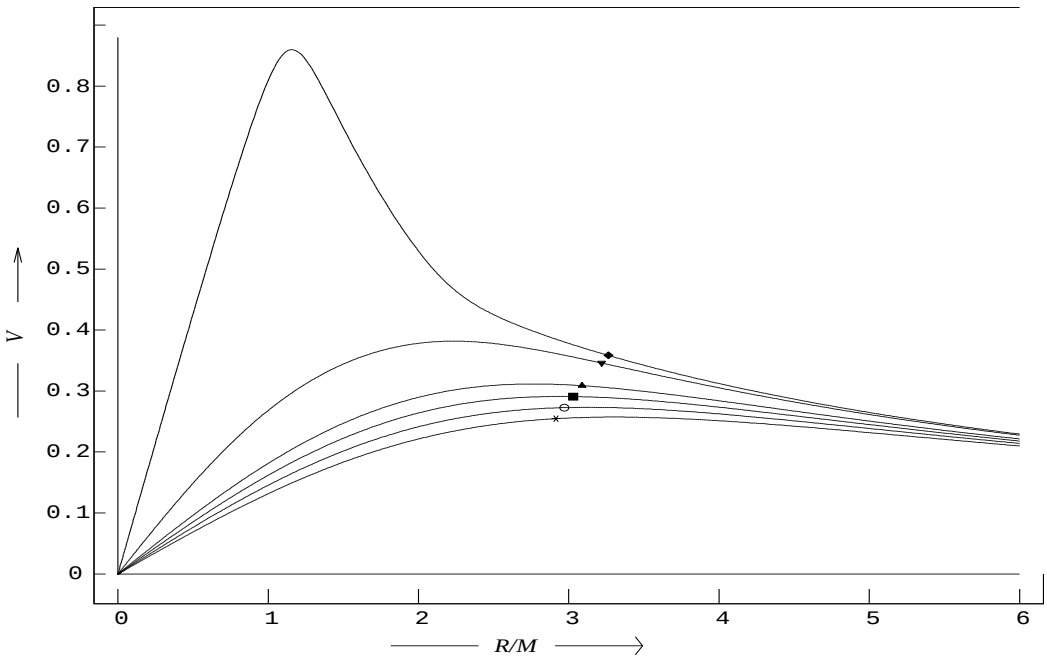

Figure 21: Velocity of ΦIOs with respect to LNRFs ($a/M = 1.1$)

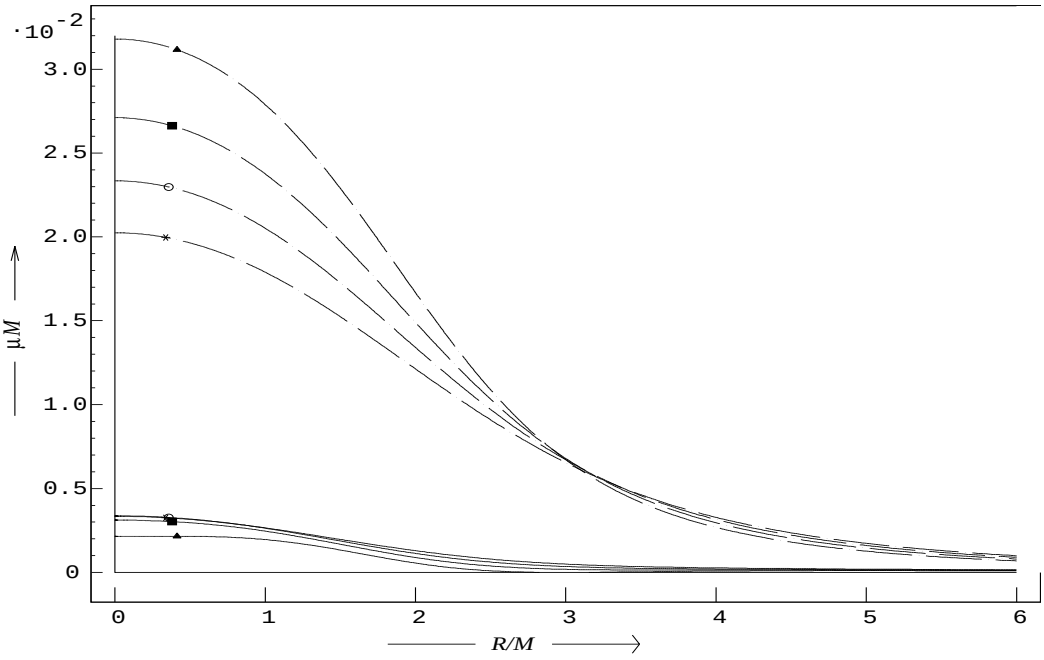

Figure 22: Energy density of both counter-rotating streams ($a/M = 1.1$)

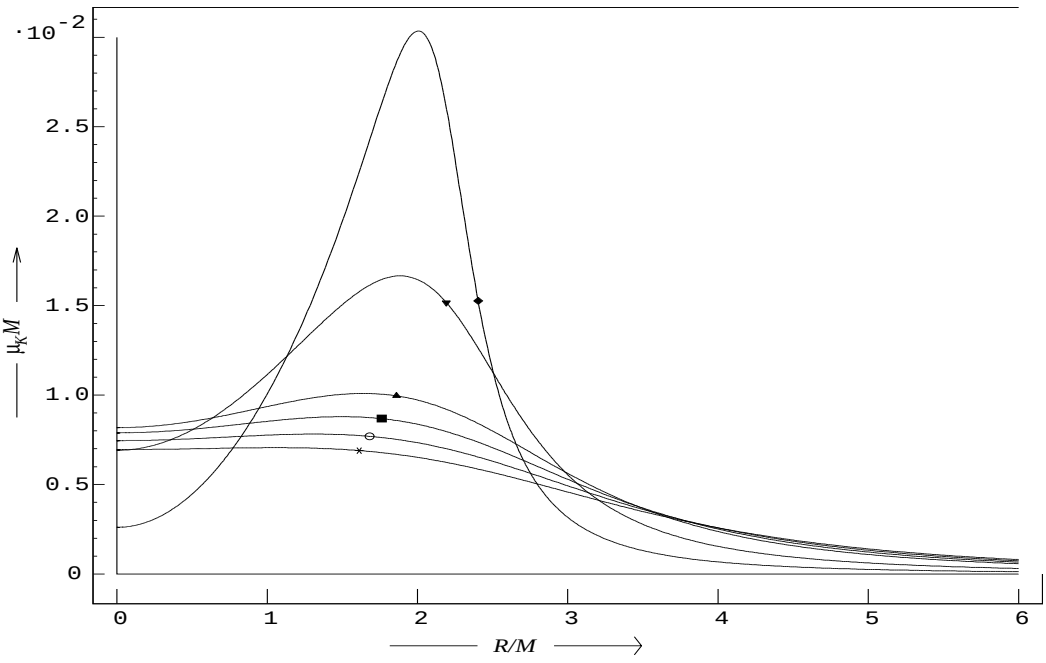

Figure 23: Komar mass density ($a/M = 1.1$)

Appendix B Radial properties of Kerr-Newman disks

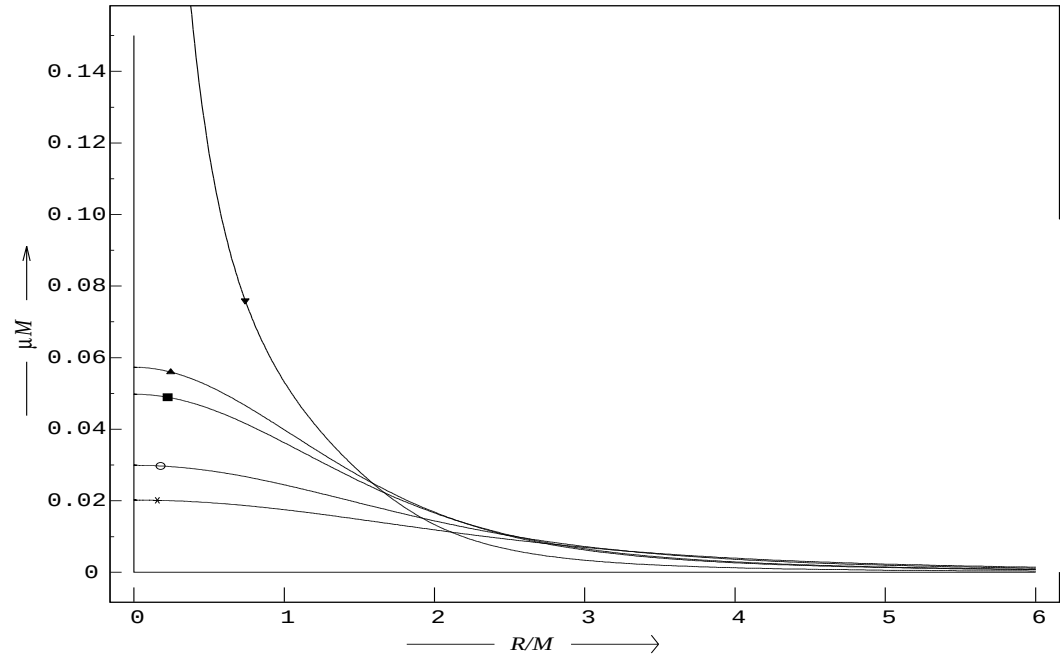

Figure 24: Energy density as seen by ΦIOs ($a/M = 0.6, Q/M = 1/\sqrt{2}$)

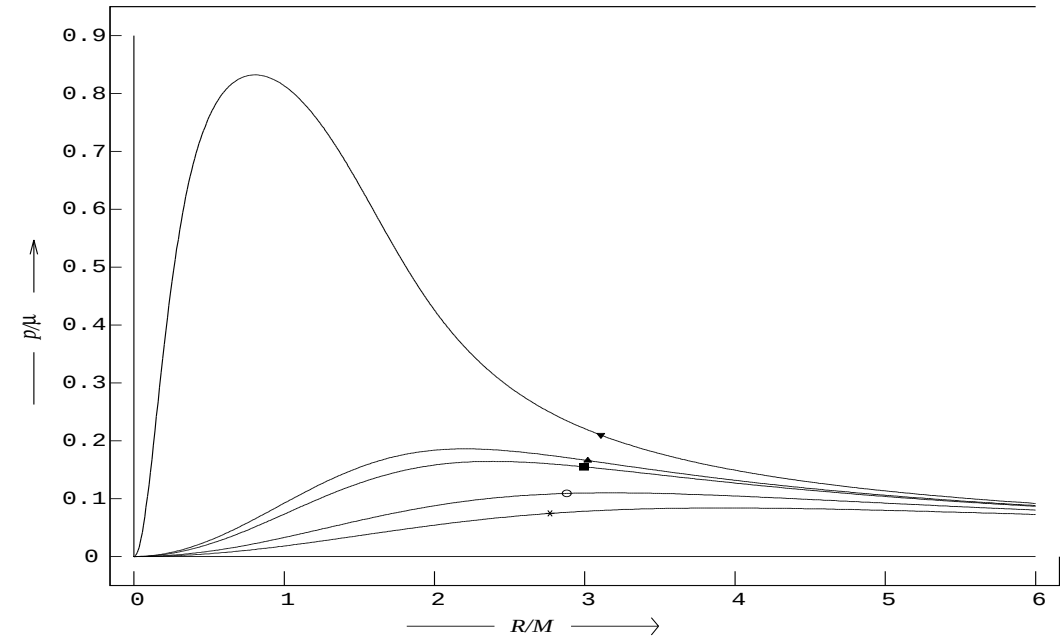

Figure 25: The ratio of the stress to the energy density as seen by ΦIOs ($a/M = 0.6$)

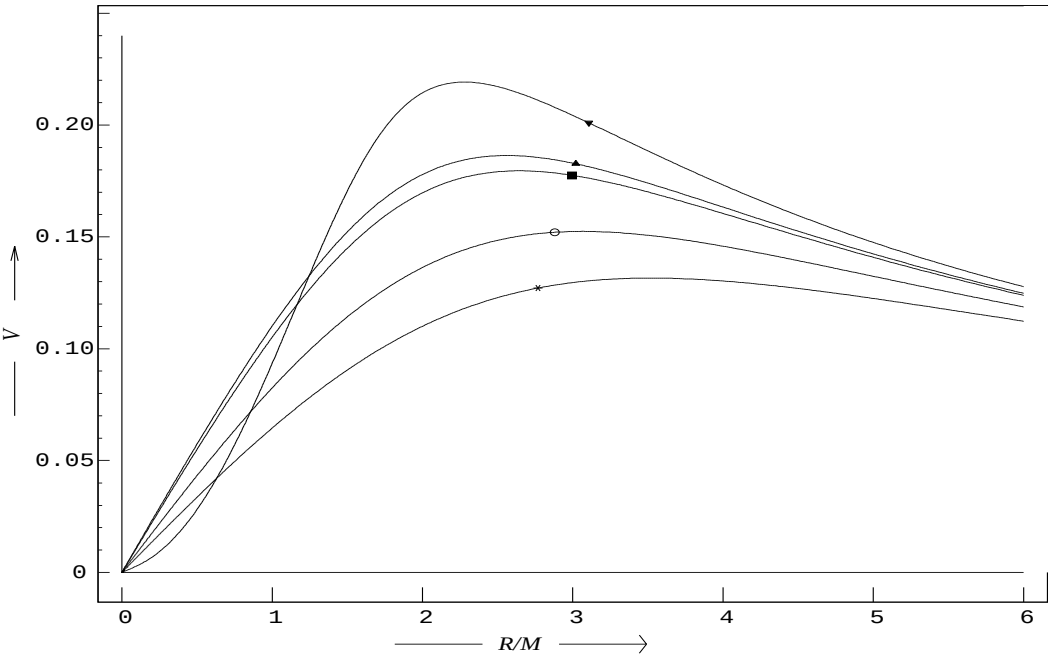

Figure 26: Velocity of ΦIOs with respect to LNRFs ($a/M = 0.6, Q/M = 1/\sqrt{2}$)

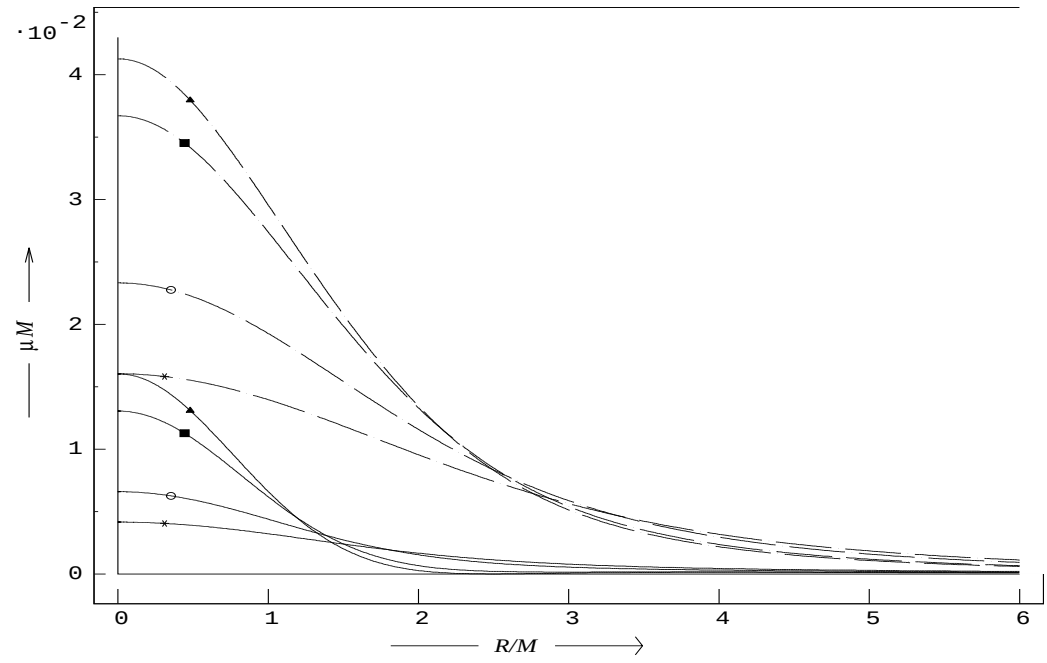

Figure 27: Energy density of both counter-rotating streams ($a/M = 0.6, Q/M = 1/\sqrt{2}$)

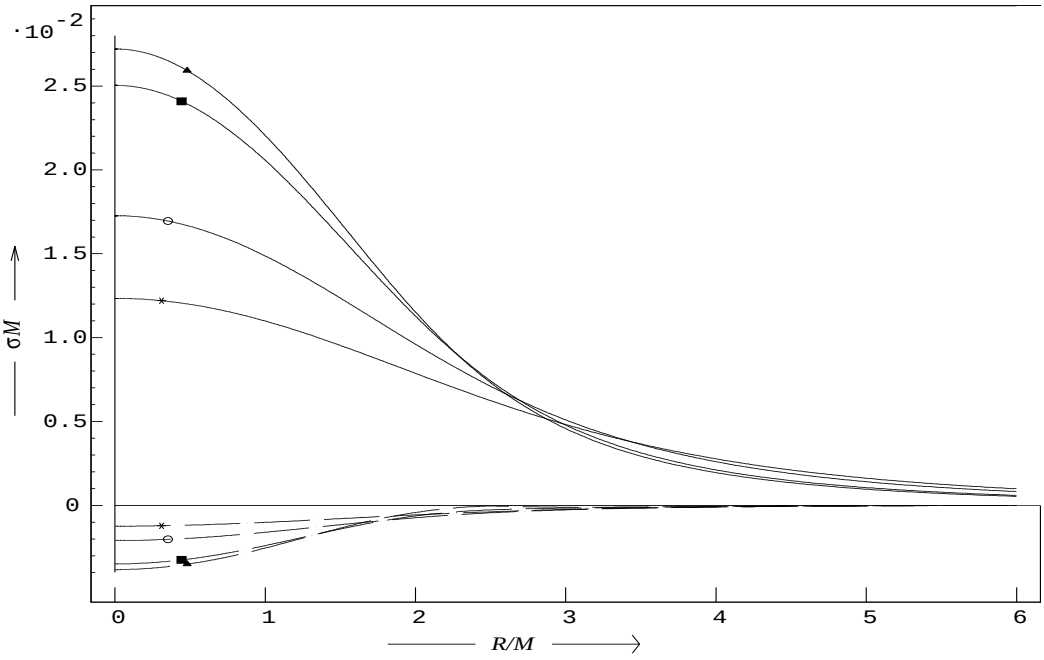

Figure 28: Charge density of both counter-rotating streams ($a/M = 0.6, Q/M = 1/\sqrt{2}$)

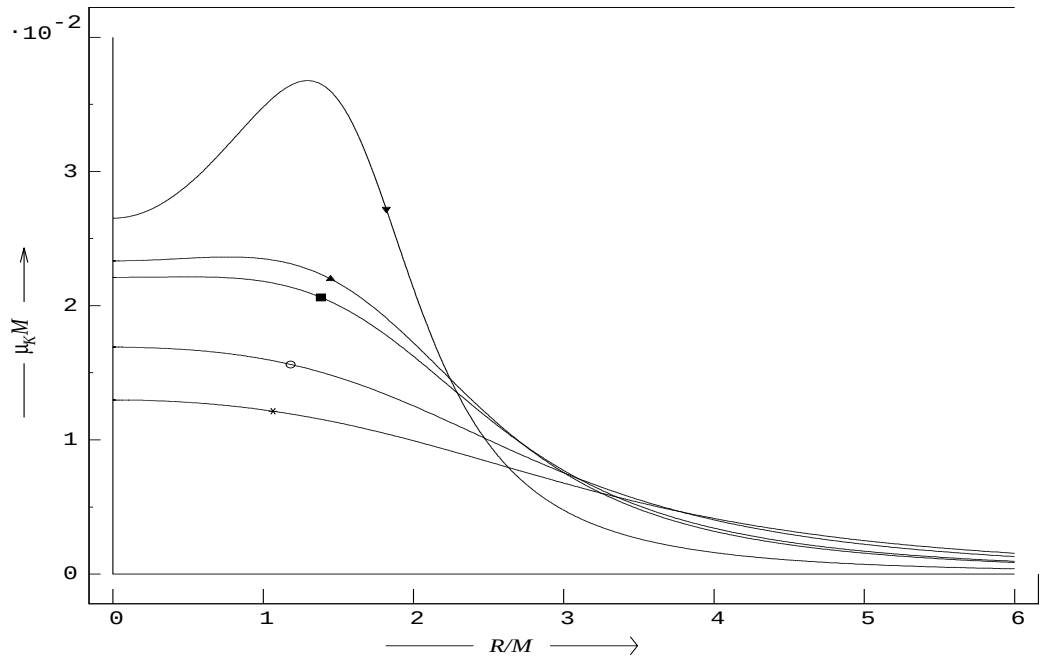

Figure 29: Komar mass density ($a/M = 0.6, Q/M = 1/\sqrt{2}$)

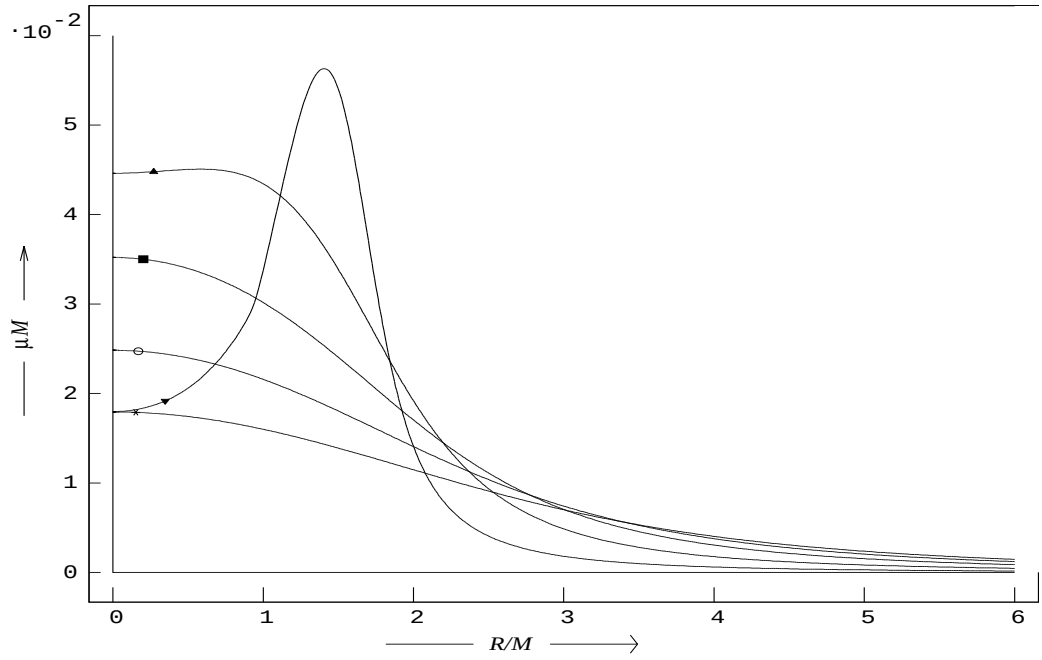

Figure 30: Energy density as seen by ΦIOs ($a/M = 0.8, Q/M = 1/\sqrt{2}$)

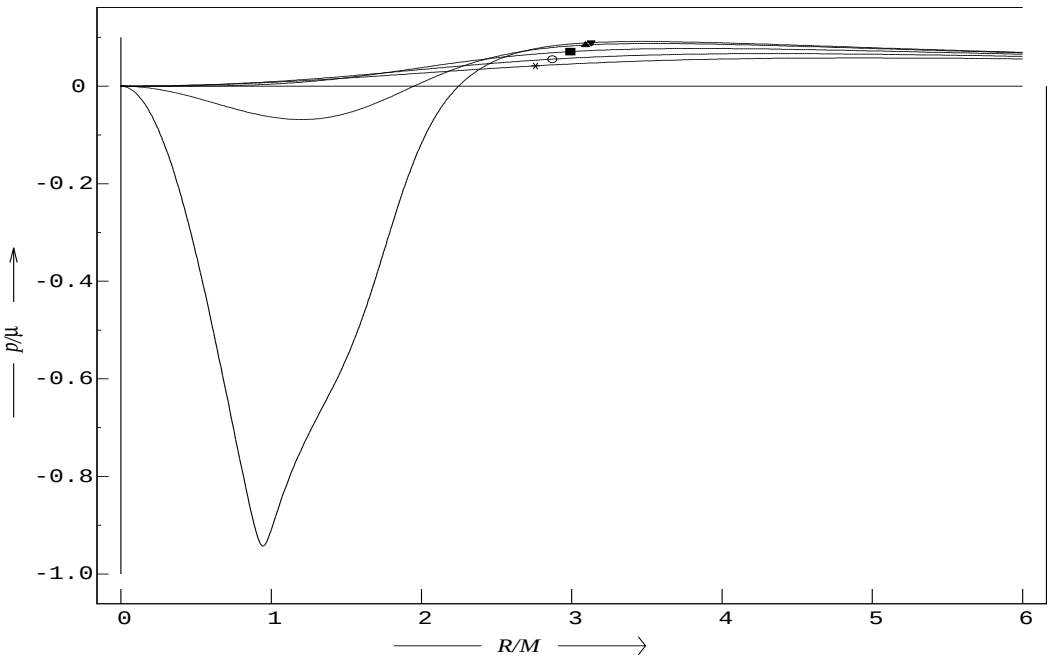

Figure 31: The ratio of the stress to the energy density as seen by ΦIOs ($a/M = 0.8$)

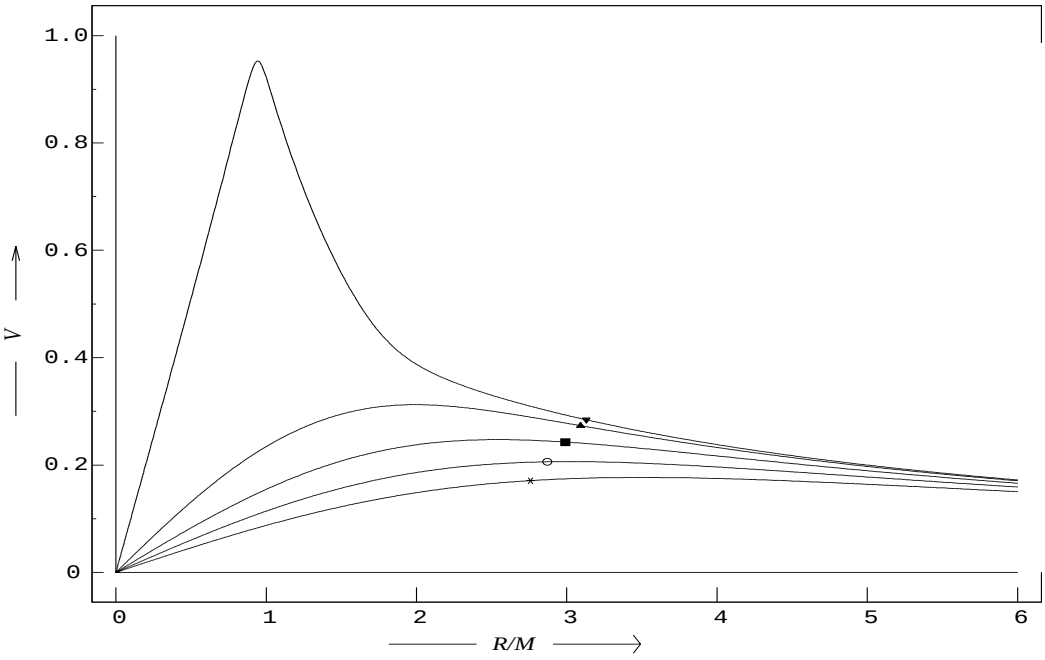

Figure 32: Velocity of ΦIOs with respect to LNRFs ($a/M = 0.8, Q/M = 1/\sqrt{2}$)

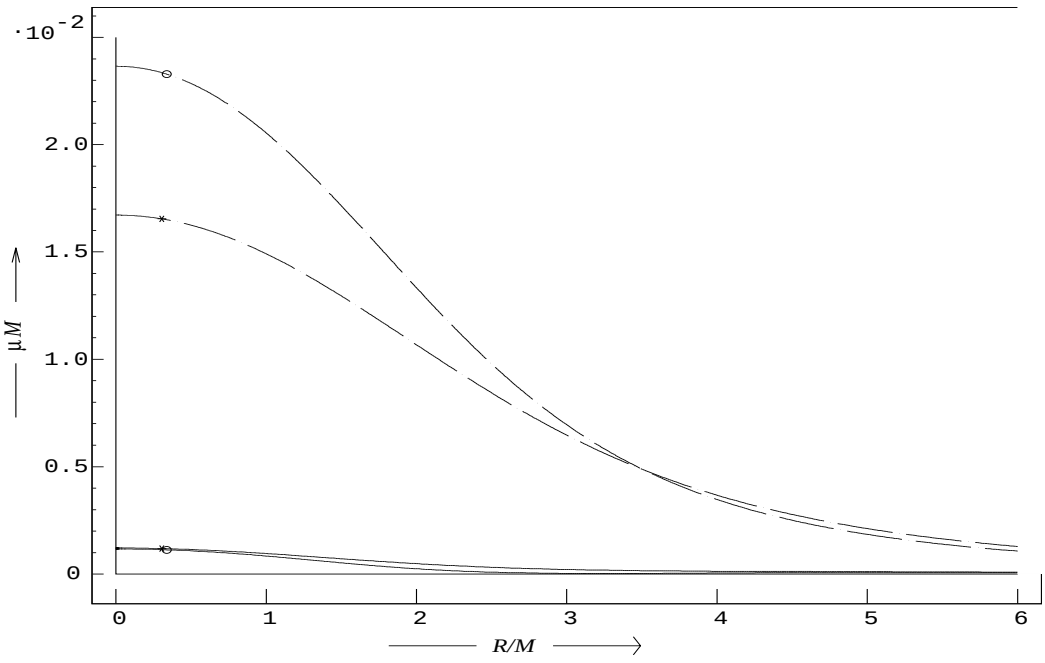

Figure 33: Energy density of both counter-rotating streams ($a/M = 0.8, Q/M = 1/\sqrt{2}$)

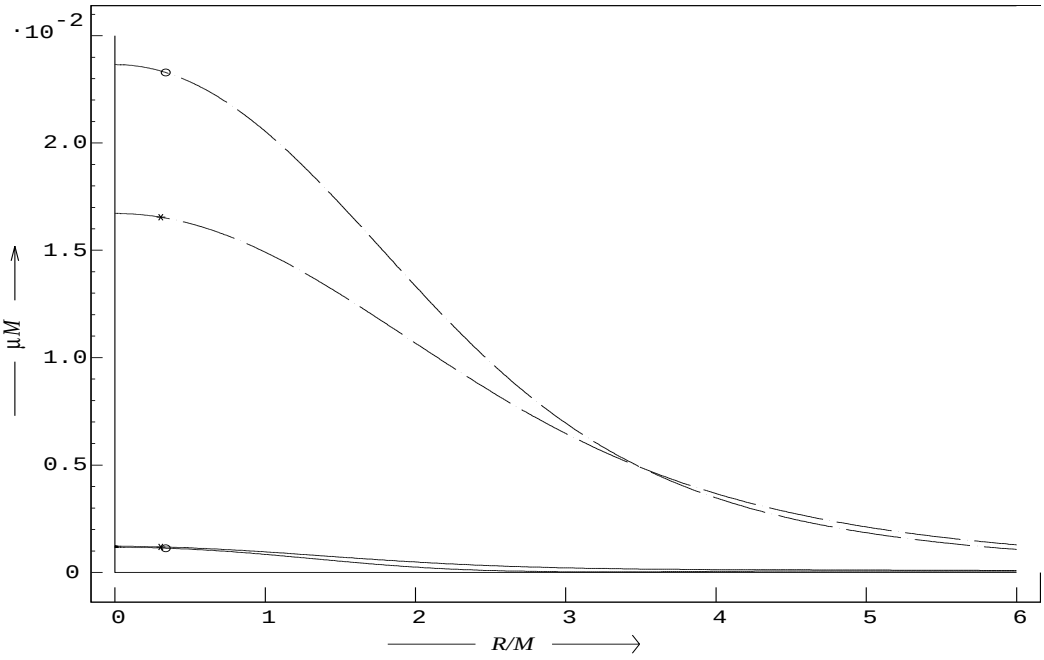

Figure 34: Charge density of both counter-rotating streams ($a/M = 0.8, Q/M = 1/\sqrt{2}$)

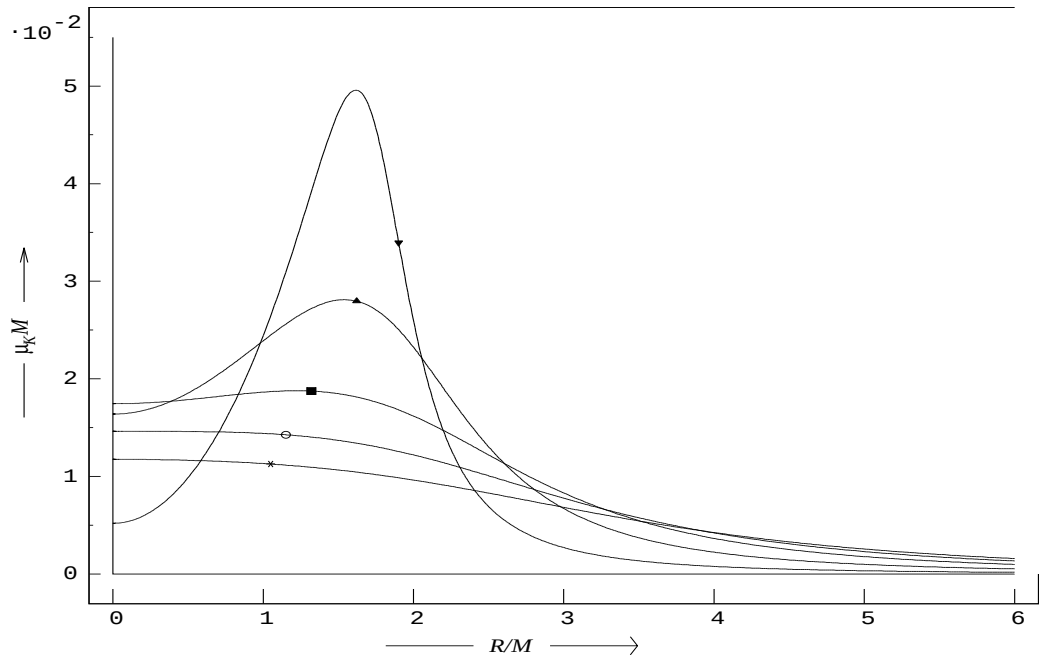

Figure 35: Komar mass density ($a/M = 0.8, Q/M = 1/\sqrt{2}$)

Appendix C Radial properties of Tomimatsu-Sato $\delta = 2$ disks

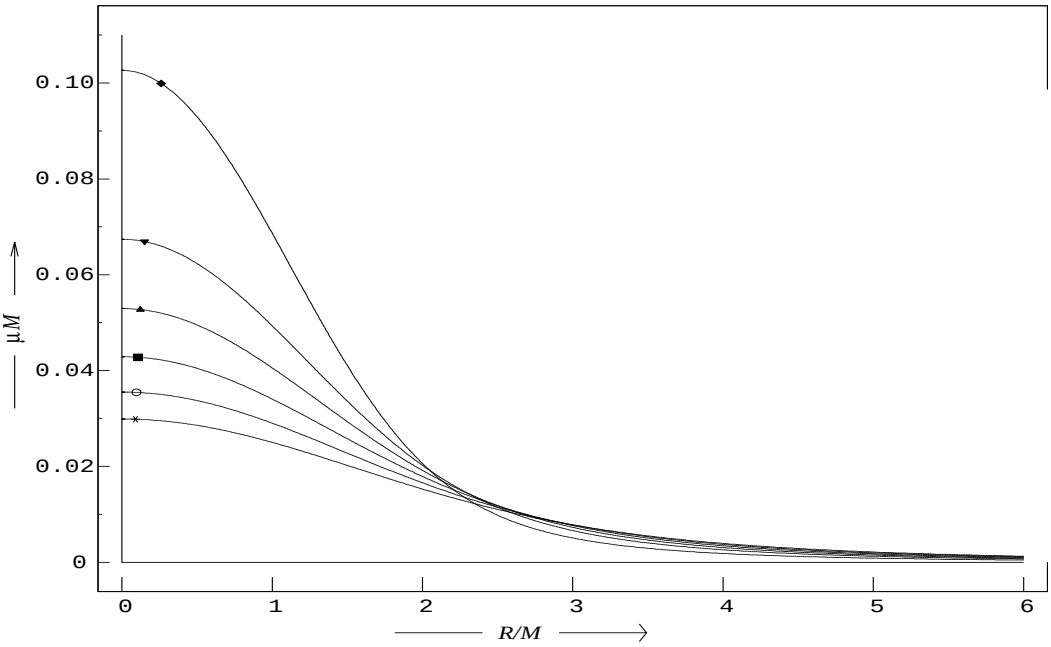

Figure 36: Energy density as seen by ΦIOs ($a/M = 0.8$)

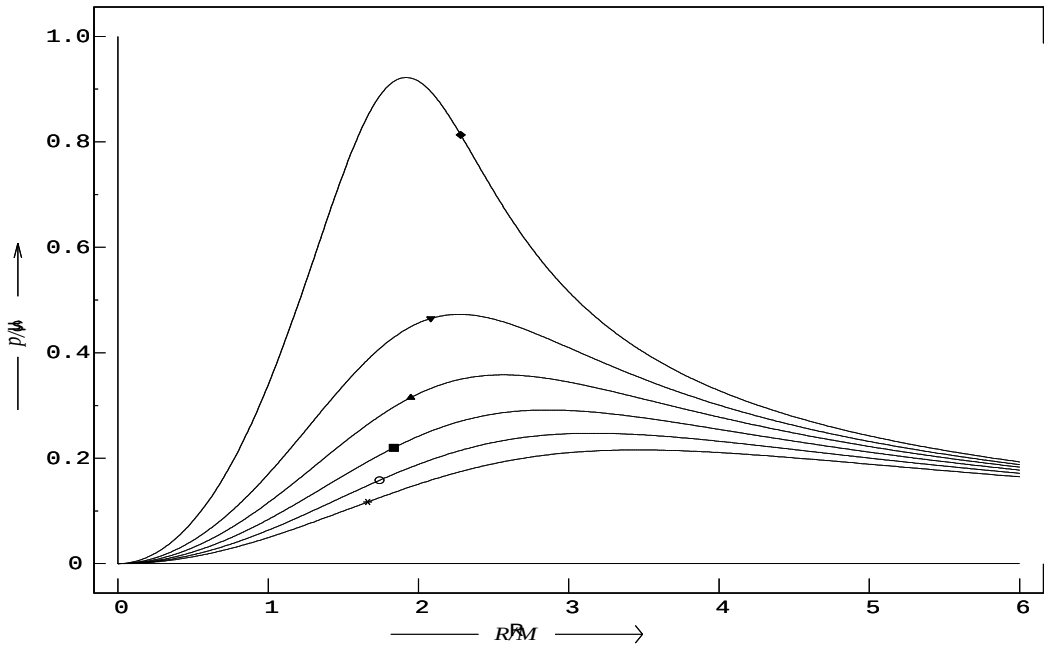

Figure 37: The ratio of the stress to the energy density as seen by ΦIOs ($a/M = 0.8$)

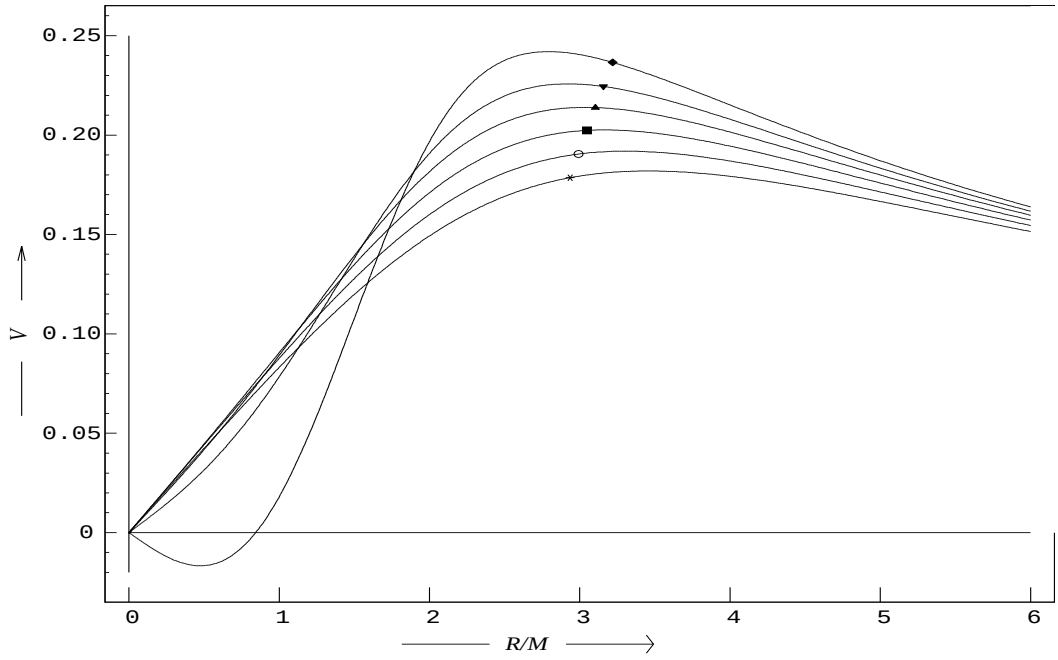

Figure 38: Velocity of the φ–isotropic observer with respect to LNRFs ($a/M = 0.8$)

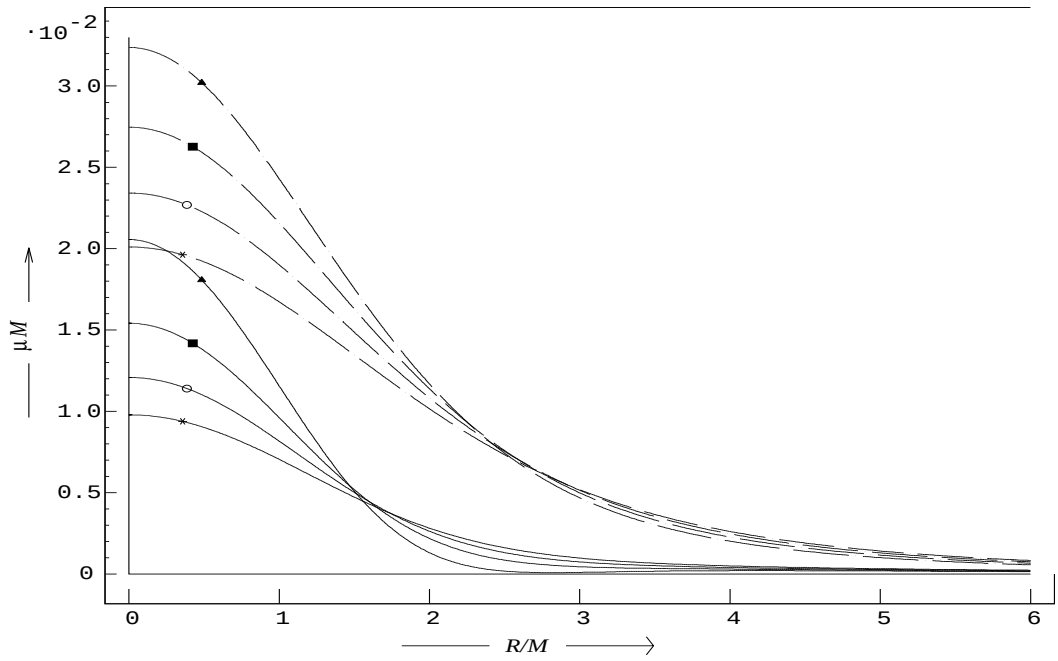

Figure 39: Energy density of both counter-rotating streams ($a/M = 0.8$)

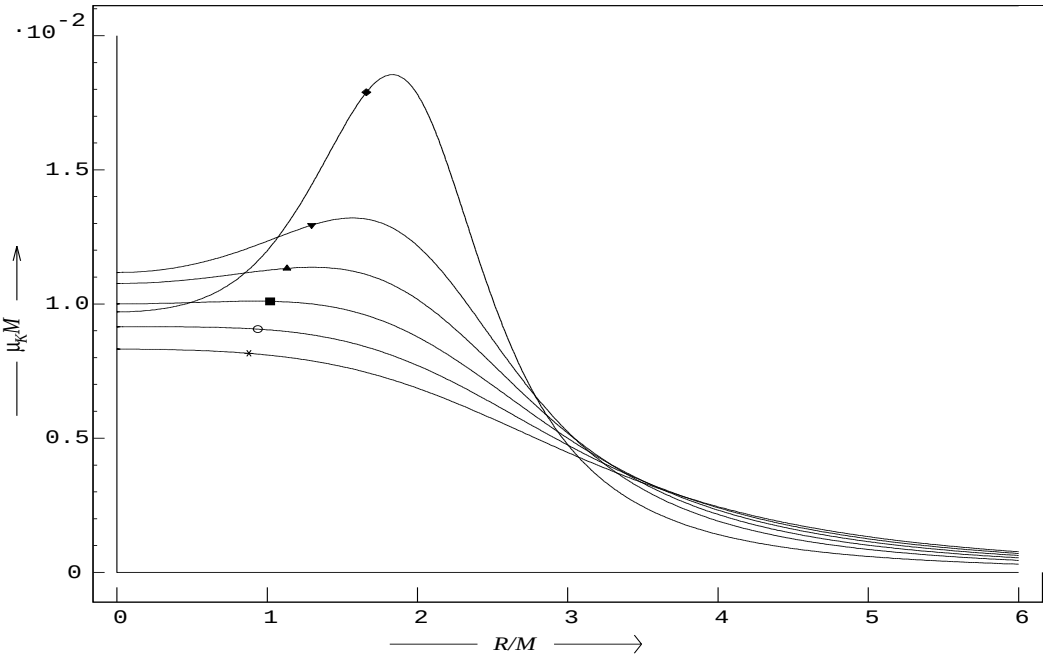

Figure 40: Komar mass density ($a/M = 0.8$)

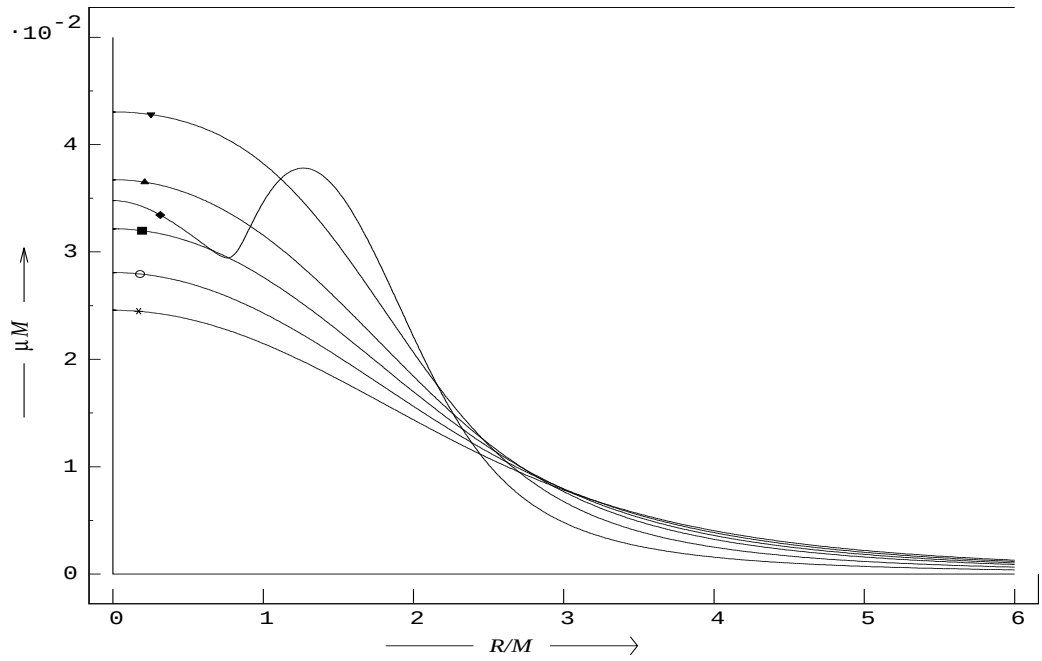

Figure 41: Energy density as seen by ΦIOs ($a/M = 1.1$)

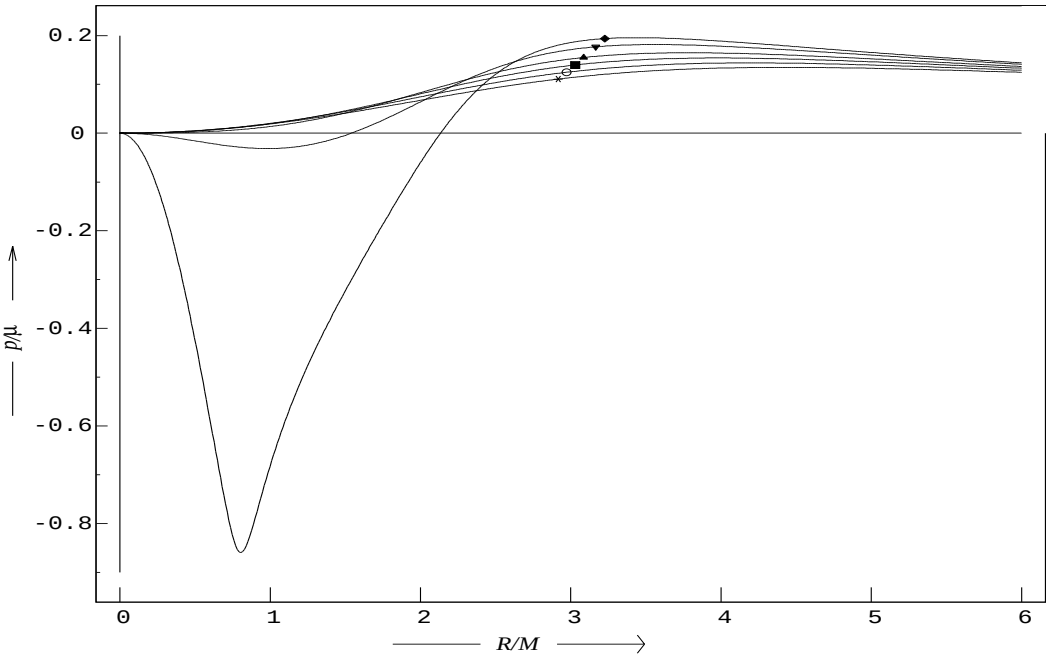

Figure 42: The ratio of the stress to the energy density as seen by ΦIOs ($a/M = 1.1$)

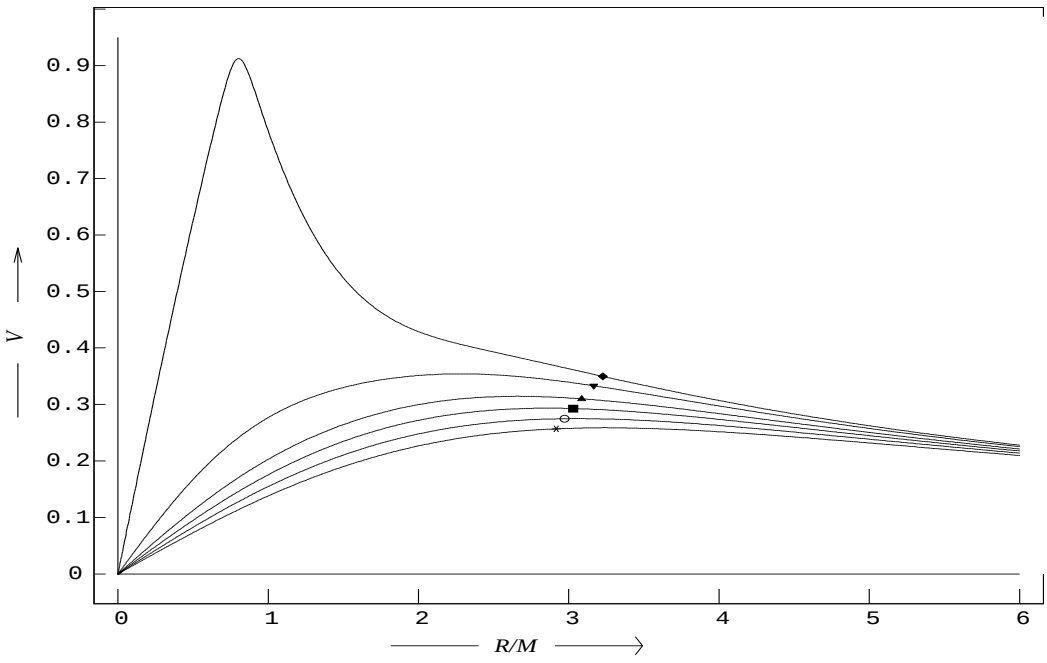

Figure 43: Velocity of ΦIOs with respect to LNRFs ($a/M = 1.1$)

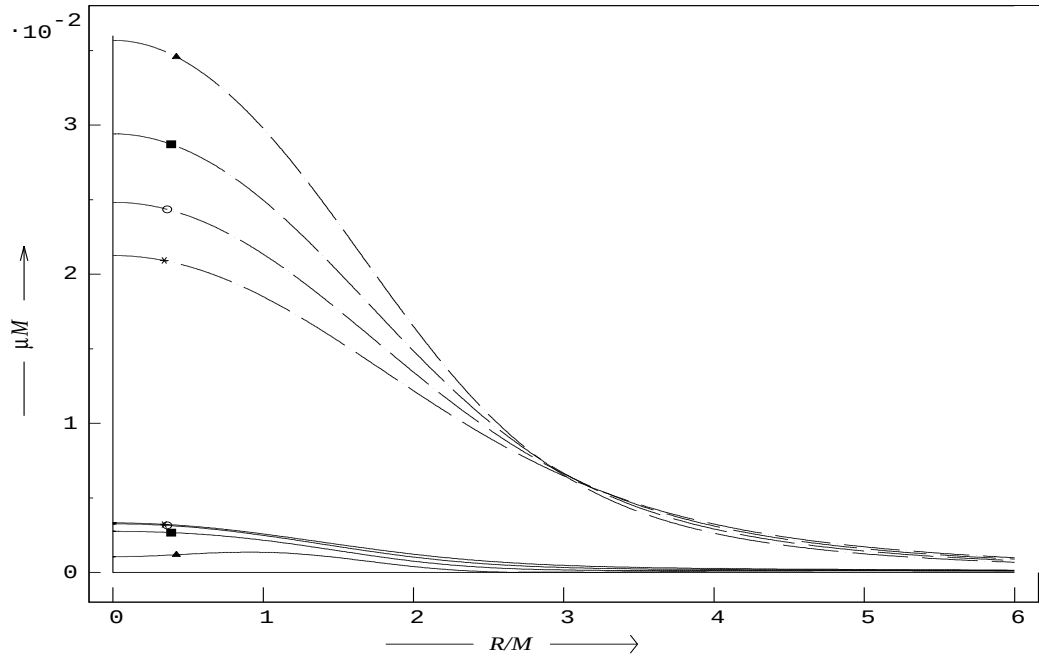

Figure 44: Energy density of both counter-rotating streams ($a/M = 1.1$)

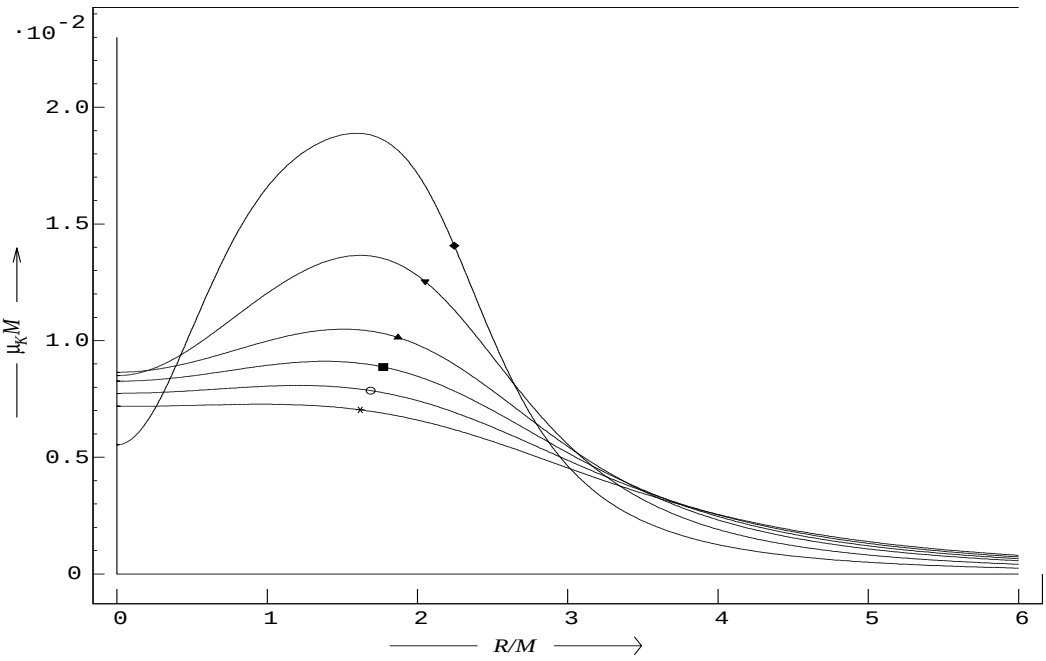

Figure 45: Komar mass density ($a/M = 1.1$)

References

[1] F. Ernst, *Phys. Rev.* **167**, 1175 (1967).

[2] R. P. Kerr, *Phys. Rev. Lett.* **11**, 237 (1963).

[3] S. Chandrasekhar, *The Role of General Relativity in Astronomy: Retrospect and Prospect*, in Highlights of Astronomy, Vol. 5, p.45, D. Reidel, Dortrecht 1980.

[4] R. M. Wald *General Relativity* (The University of Chicago Press, Chicago, 1984).

[5] M. A. Abramowitz and S. Sonego, Abstracts of JENAM98 p. 265, Prague, 1998.

[6] E. T. Newman and A. I. Janis, *J. Math. Phys.* **6**, 915 (1965).

[7] R. H. Boyer and R. W. Lindquist, *J. Math. Phys.* **8**, 265 (1967).

[8] W. Hernandez, *Phys. Rev.* **159**, 1070 (1967).

[9] M. A. Abramowitz, J. P. Lasota and B. Muchotrzeb, *Commun. Math. Phys.* **47**, 109 (1976).

[10] J. Marek and A. Sloane, *Nuov. Cim.* B **51**, 45 (1979).

[11] D. Balaba, *Gen. Rel. and Grav.* **18**, 173 (1986).

[12] C. A. López, *Nuov. Cim.* B **66**, 17 (1981).

[13] S. P. Drake and R. Turola, *Class. Quantum Grav.* **14**, 1883 (1997).

[14] D. McManus, *Class. Quantum Grav.* **8**, 863 (1991).

[15] A. Krasiński, *Annals of Physics* **112**, 22 (1978).

[16] M. A. Abramowitz, W. Arkuszewski and B. Muchotrzeb, *Lett. Nuov. Cim.* **15**, 477 (1976).

[17] J. M. Bardeen and R. V. Wagoner, *Astrophys. J.* **167**, 359 (1971)

[18] G. Neugebauer and R. Meinel, *Astrophys. J.* **414**, L97 (1993)

[19] J. Bičák and T. Ledvinka, *Phys. Rev. Lett.* **71**, 1669 (1993).

[20] Z. Y. Turakulov, *Mod. Phys. Lett.* A **5**, 725 (1990).

[21] V. C. Rubin, J. A. Graham and J. D. P. Kenney, *Astrophys. J.* **394**, L9 (1992)

[22] J. Bičák and D. Lynden-Bell, and J. Katz, *Phys. Rev.* D **47**, 4334 (1993).

[23] J. Binney and S. Tremaine, *Galactic Dynamics*, (Princeton University Press, Princeton 1987).

[24] G. G.Kuzmin, *Astr.Zh.* **33**,27 (1956).

[25] J. Bičák and D. Lynden-Bell, and C. Pichon, *MNRAS* **265**, 126 (1993).

[26] N. W. Evans and P.T. de Zeeuw, *Mon. Not. R. Astr. Soc.* **257**, 152 (1992).

[27] D.Krammer, H. Stephani, M. MacCallum, and E.Herlt, *Exact solutions of Einstein's Field Equations* (Cambridge University Press, Cambridge, 1980).

[28] C. Barabès and W. Israel, *Phys.Rev.D* **43**,1129 (1991).

[29] W. Israel, *Nuov. Cim.* **44**, 1 (1966); **48**, 463 (1967).

[30] K. Kuchař, *Czech J. Phys.*B **18**, 435 (1968).

[31] C. Pichon and D. Lynden-Bell, *MNRAS* **280**, 1007 (1996).

[32] C. A. López, *Nuov. Cim.* B **76**, 9 (1983).

[33] T. Morgan and L.Morgan, *Phys. Rev.* **183**, 1097 (1969).

[34] Z. Perjés, *J. Math. Phys.* **30**, 2197 (1989).